

2001

Petrology of Eocene carbonates in the Wasatch Formation, Southwestern Wyoming

John Robert Hawk
San Jose State University

Follow this and additional works at: https://scholarworks.sjsu.edu/etd_theses

Recommended Citation

Hawk, John Robert, "Petrology of Eocene carbonates in the Wasatch Formation, Southwestern Wyoming" (2001). *Master's Theses*. 2181.

DOI: <https://doi.org/10.31979/etd.68tp-bnaf>

https://scholarworks.sjsu.edu/etd_theses/2181

This Thesis is brought to you for free and open access by the Master's Theses and Graduate Research at SJSU ScholarWorks. It has been accepted for inclusion in Master's Theses by an authorized administrator of SJSU ScholarWorks. For more information, please contact scholarworks@sjsu.edu.

INFORMATION TO USERS

This manuscript has been reproduced from the microfilm master. UMI films the text directly from the original or copy submitted. Thus, some thesis and dissertation copies are in typewriter face, while others may be from any type of computer printer.

The quality of this reproduction is dependent upon the quality of the copy submitted. Broken or indistinct print, colored or poor quality illustrations and photographs, print bleedthrough, substandard margins, and improper alignment can adversely affect reproduction.

In the unlikely event that the author did not send UMI a complete manuscript and there are missing pages, these will be noted. Also, if unauthorized copyright material had to be removed, a note will indicate the deletion.

Oversize materials (e.g., maps, drawings, charts) are reproduced by sectioning the original, beginning at the upper left-hand corner and continuing from left to right in equal sections with small overlaps.

Photographs included in the original manuscript have been reproduced xerographically in this copy. Higher quality 6" x 9" black and white photographic prints are available for any photographs or illustrations appearing in this copy for an additional charge. Contact UMI directly to order.

ProQuest Information and Learning
300 North Zeeb Road, Ann Arbor, MI 48106-1346 USA
800-521-0600

UMI[®]

NOTE TO USERS

This reproduction is the best copy available.

UMI

**PETROLOGY OF EOCENE CARBONATES
IN THE WASATCH FORMATION,
SOUTHWESTERN WYOMING**

A Thesis

Presented to

The Faculty of the Department of Geology

San Jose State University

In Partial Fulfillment

of the Requirements for the Degree

Master of Science

By

John Robert Hawk

July 2001

UMI Number: 1405503

Copyright 2001 by
Hawk, John Robert

All rights reserved.

UMI[®]

UMI Microform 1405503

Copyright 2001 by Bell & Howell Information and Learning Company.

All rights reserved. This microform edition is protected against
unauthorized copying under Title 17, United States Code.

Bell & Howell Information and Learning Company
300 North Zeeb Road
P.O. Box 1346
Ann Arbor, MI 48106-1346

© 2001

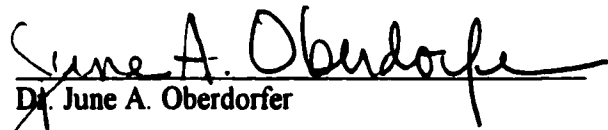
John Robert Hawk

ALL RIGHTS RESERVED

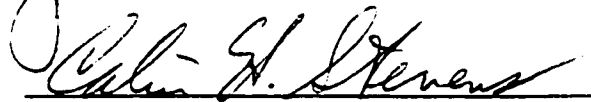
APPROVED FOR THE DEPARTMENT OF GEOLOGY



Dr. David W. Andersen

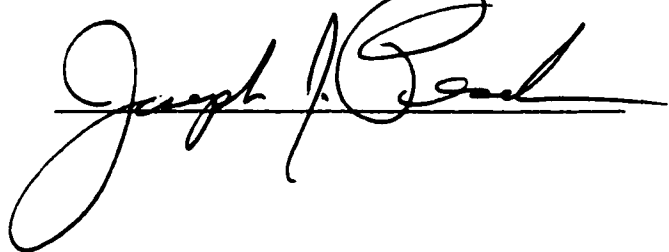


Dr. June A. Oberdorfer



Dr. Calvin H. Stevens

APPROVED FOR THE UNIVERSITY



ABSTRACT

PETROLOGY OF EOCENE CARBONATES IN THE WASATCH FORMATION, SOUTHWESTERN WYOMING

By John R. Hawk

Study of three limestone beds from a portion of the main body of the Wasatch Formation (Eocene) within the Washakie Basin, Sweetwater County, Wyoming indicates that these limestones were deposited in floodplain ponds. Lab work on samples from these beds included X-ray, insoluble residue and petrographic analysis. The limestone beds consist primarily of biomicrites, with five samples that are fossiliferous micrites. A small fossil assemblage and low amounts of siliciclastics characterize bed #1, which implies a fairly stable pond environment. Bed #2 contains a diverse invertebrate fossil assemblage, the vertebrate *Stickleback* and variable low to high amounts of siliciclastics, suggesting a quiet, very stable pond environment. Bed #3 has low amounts of siliciclastics and an intermediate fossil assemblage, and it is interpreted as a stable to fairly stable pond environment. Both the field and lab data show that each bed is distinctive and easily recognized throughout the field area.

ACKNOWLEDGMENTS

The author is grateful to David W. Andersen (San Jose State University) who served as chairman of the Master's thesis committee and who provided direction and guidance throughout the project. The writer is also grateful to June Oberdorfer (San Jose State University) and Cal Stevens (San Jose State University), who also served on the graduate committee and provided their time and valuable suggestions concerning the manuscript.

The author gives special thanks to his good friend Mark Sabiers, who accompanied him into the field and was of great assistance in collecting samples and measuring sections. Thanks also go to LB, who helped organize the different data that were generated during the analysis of the carbonate samples. Further thanks go to my mother Sally and my sister Barbara who helped in the preparation of rock samples for crushing and analysis. I regret that I was unable to finish this thesis prior to my sister Barbara passing away a year and a half ago; I know that she was looking forward to the day that I finished my thesis. I will miss her at the graduation ceremony.

Lastly, the author wishes to express his deepest thanks to his wife Diane, who gave endless moral support and patiently stood by me as I endeavored to finish this thesis. I look forward to having some "free time" now that this project is complete!

TABLE OF CONTENTS

	Page
INTRODUCTION	1
GEOLOGIC SETTING	5
Regional Stratigraphy	5
Eocene Climate	7
Structural History	8
Local Stratigraphy and Paleoenvironment	9
METHODS	11
Field Procedure	11
Laboratory Procedure	15
X-ray Diffraction	15
Insoluble Residue	18
Petrography	18
RESULTS	20
Stratigraphy	20
Limestone #1	20
Limestone #2	22
Limestone #3	24
Laboratory Analysis	25
X-ray Diffraction	28
Insoluble Residue	29
Petrography	32
Comparison of Data Sets	48

FOSSILS	52
DISCUSSION	54
Depositional Environment	54
General Overview	56
Bed #1	59
Bed #2	60
Bed #3	62
Summary	64
Distinctive Features of Beds	65
CONCLUSIONS	67
REFERENCES CITED	69
APPENDIX A: DESCRIPTION OF MEASURED SECTIONS	73
Section 1	73
Section 2	74
Section 3	76
Section 4	77
APPENDIX B: X-RAY DIFFRACTION DATA	79
APPENDIX C: INSOLUBLE RESIDUE DATA	81
APPENDIX D: PETROGRAPHIC DATA.....	82

LIST OF ILLUSTRATIONS

Figure	Page
1. Index Map of Wyoming	2
2. Location Map of Field Area	3
3. Stratigraphic Correlation Diagram	6
4. Map Showing Measured Sections	12
5. Photograph of Measured Sections #1 and #2	13
6. Photograph of Measured Section #2	13
7. Photograph of Measured Sections #3 and #4	14
8. Topographic Map Showing Locations of Samples	16
9. Measured Sections #1 - #4, Showing Stratigraphic Relationships	21
10. Residue versus Distance from Eastern Edge of Field Area	30
11. Photomicrograph of Biomicrite in Bed #1	33
12. Photomicrograph of Biomicrite in Bed #2	33
13. Photomicrograph of Biomicrite in Bed #3	34
14. Photomicrograph of <i>Biomphalaria</i>	34
15. Total Fossils versus Matrix	36
16. Total Fossils versus Non-carbonate Grains	37
17. Total Fossils versus Residue	40
18. Pelecypods versus Gastropods	41
19. Total Fossils versus Distance from Eastern Edge of Field Area	43
20. Ostracods, Gastropods and Pelecypods as Percent of Total Sample	45
21. Abundances of Intact and Fragmented Fossils and Non-carbonate Components	47

LIST OF TABLES

Table	Page
1. Master Table of X-ray, Residue and Point Count Data	26
2. Table of Identified Fossils in Each Bed	53

INTRODUCTION

During the Eocene epoch, an extensive intermontane basin system existed over much of Wyoming, Colorado and Utah (Fig. 1). The basins were rimmed by Precambrian-cored uplifts and were filling with fluvial and lacustrine deposits.

Savage and others (1972) reported the occurrence of a remarkably diverse suite of vertebrate fossils within the Eocene Wasatch Formation along the western margin of the Washakie Basin in southern Wyoming (Figs. 1 and 2). These fossils occur in fluvial channel sandstones, fine-grained interchannel deposits, and thin limestone beds that formed on the floodplain. The laterally extensive limestone beds also contain diverse invertebrate fossil assemblages. The fossil vertebrate localities occur at many stratigraphic levels and at widely spaced locations along the strike of the beds, so that detailed correlation of the sites had been difficult. The laterally extensive limestone beds probably offer the best opportunity for correlation (Savage and others, 1972; Roehler, 1977; Roehler and Valcarce, 1978).

This study focused on three of these limestone beds in an attempt to identify possible definitive characteristics that could be used for identification. Detailed analysis of carbonate samples and measured sections was used to evaluate which features of the carbonates are most useful to differentiate them from one another, both in the field and by laboratory analysis, and to determine the extent of variation within each bed. Laboratory work included X-ray, insoluble residue and petrographic analysis. These limestones were deposited upon a floodplain in an intermontane basin and the interbedded siliciclastics were deposited mostly by streams within this basin (Roehler, 1979).

One goal of this study was to ascertain if the properties of the beds and their included fossil assemblages could be used to interpret the local depositional

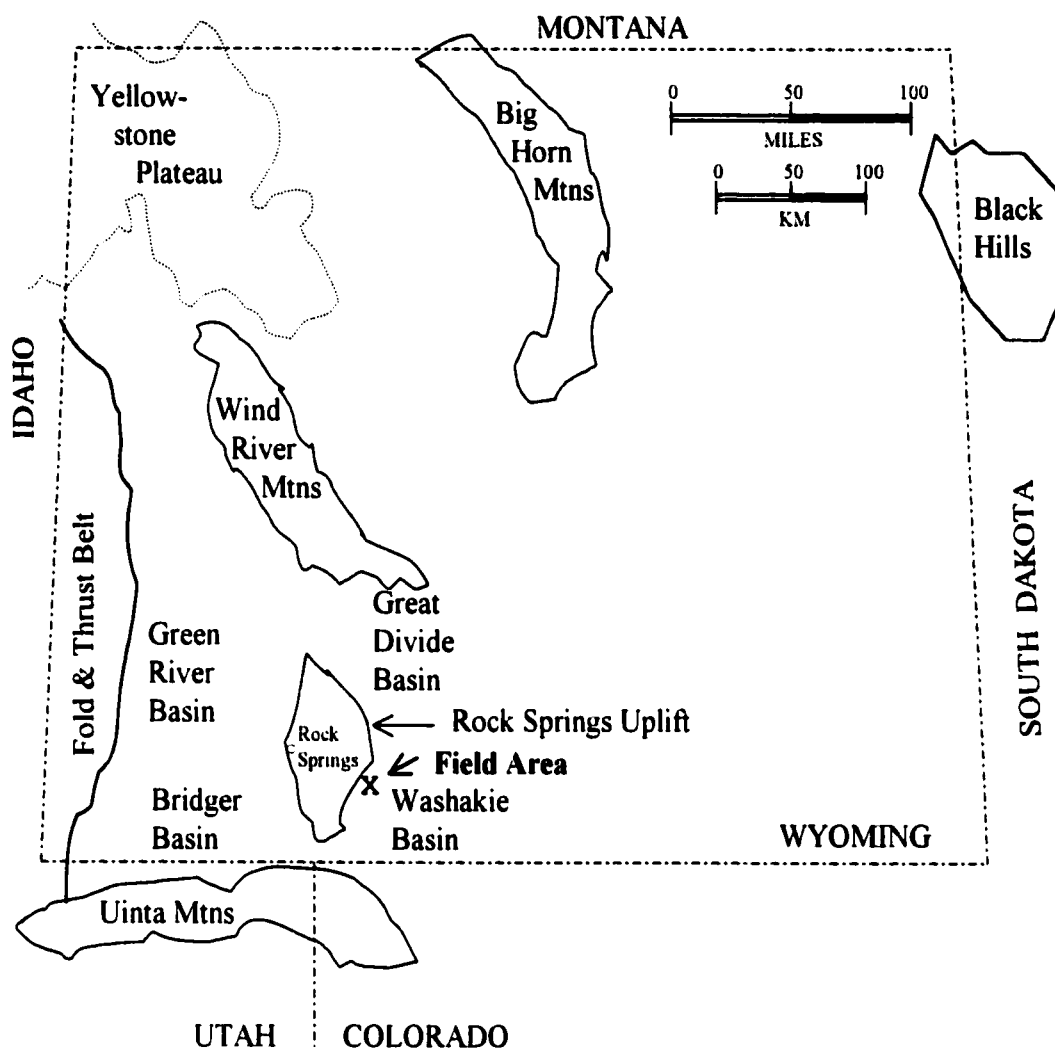


Figure 1: Index map of Wyoming foreland showing approximate location of field area. Modified from Wray (1988).

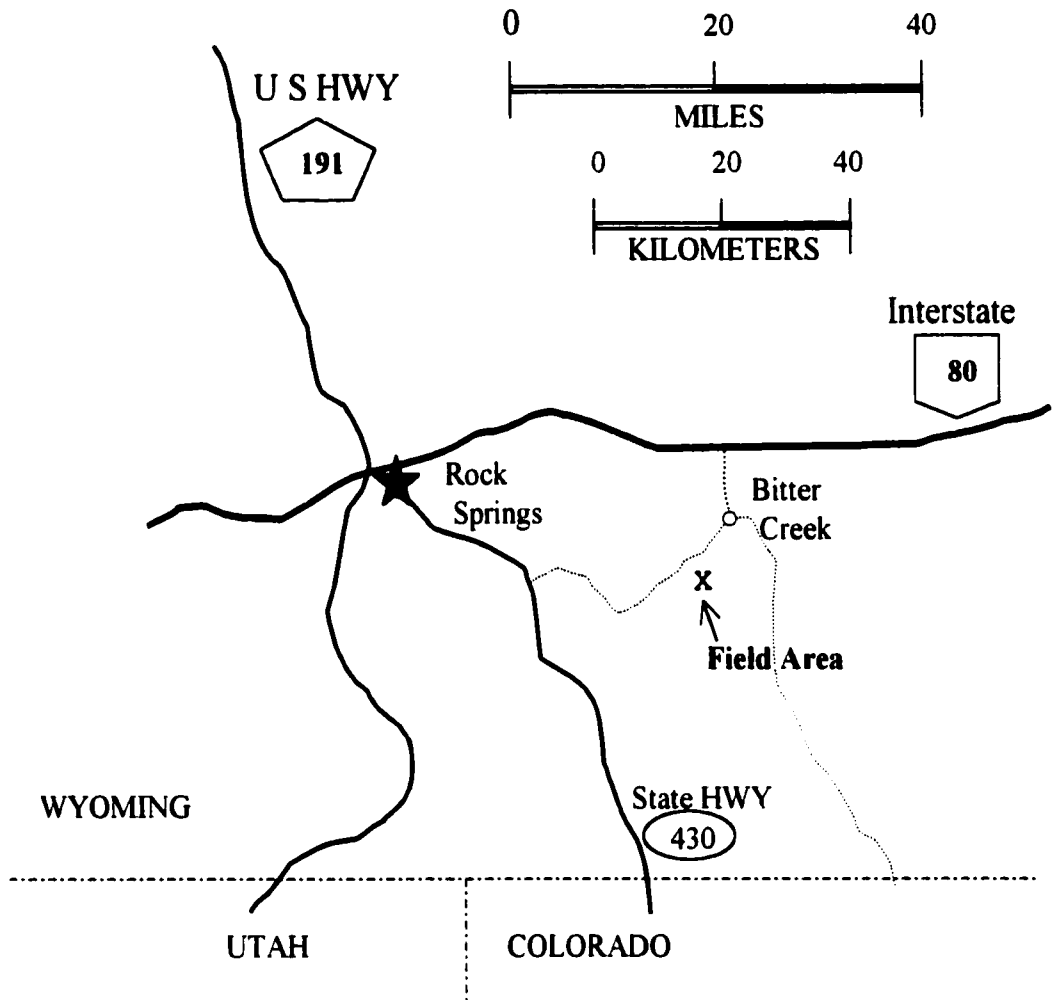


Figure 2: Location map of field area showing roads and state boundaries (dash-dot lines).

environments and any lateral changes within the beds. Another goal was to determine whether or not these three limestone beds can be distinguished in the field and if each is consistently identifiable along the strike of the bed. Properties determined in the laboratory are also evaluated to determine whether or not they are internally consistent and distinguishable for each of the three beds.

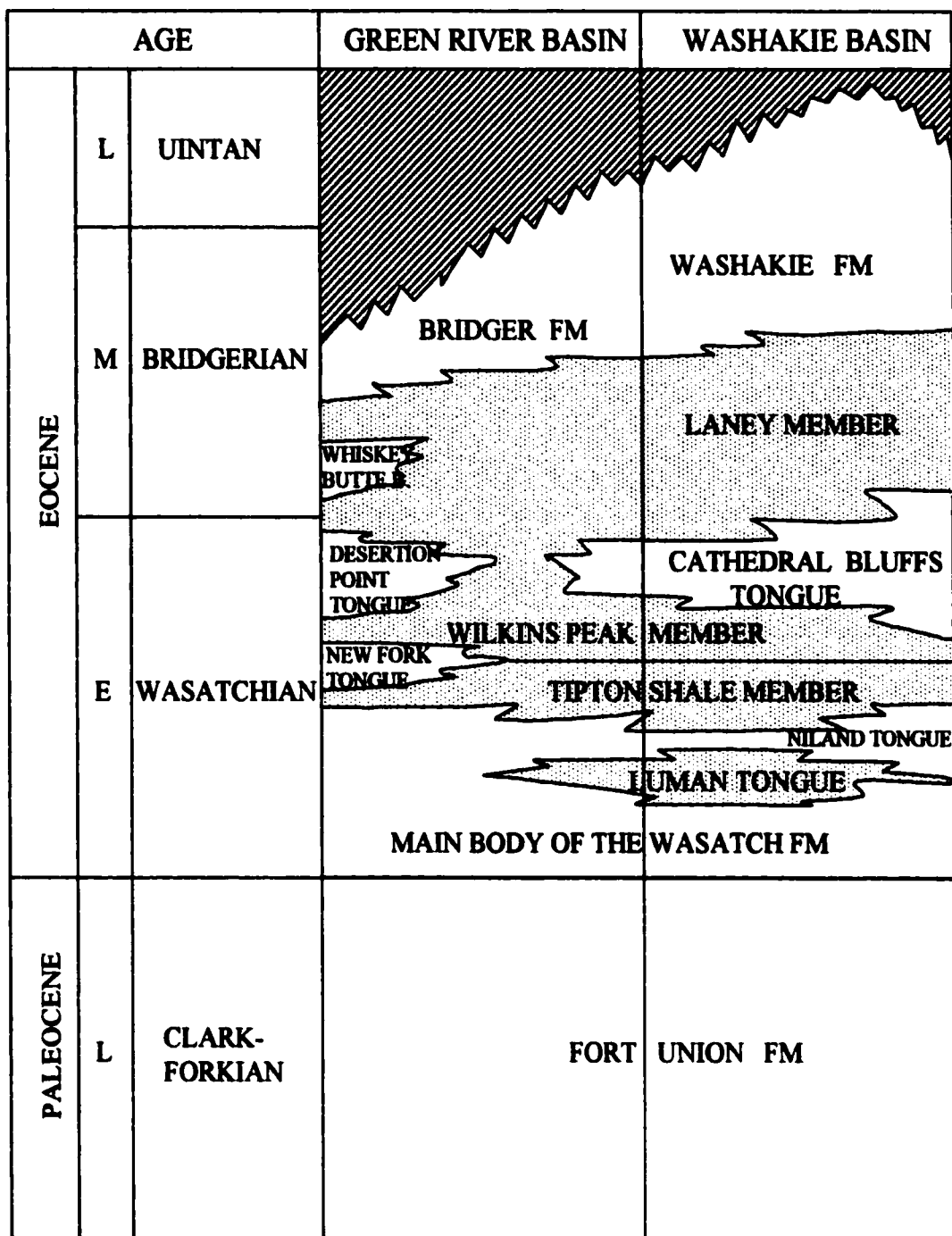
GEOLOGIC SETTING

Regional Stratigraphy

The Eocene Wasatch Formation is widely distributed in southwestern Wyoming and is made up of several tongues that interfinger with various members of the Green River Formation (Fig. 3). The part of the Wasatch that underlies the lowest tongue of the Green River Formation is called the main body of the Wasatch Formation and is the subject of this report. The thickness of the main body of the Wasatch Formation is approximately 550 m and the Green River Formation is about 1000 m thick (Sullivan, 1980).

The Wasatch Formation is composed of predominantly fluvial rocks, and the dominant lithologies are sandstone and mudstone. Sullivan (1980) recognized three main facies: the red-bed fluvialite, the pediment, and the non-red fluvialite-paludal facies. Limestone and marlstone also are interbedded within the main body of the Wasatch Formation. These facies commonly show dramatic variations and gradations in lithology and color when traced along the strike of the bed.

The overlying and interfingering Green River Formation consists mostly of the lacustrine deposits of Lake Gosuite. The extent of this lake fluctuated widely over the life of the lake (Bradley, 1964; Sullivan, 1980), producing a variety of organic-rich alkaline-earth carbonate and trona deposits, fine-grained clastic beds, sandstones, algal- and mollusc-bearing limestones, thin-bedded carbonates, cherts and low-grade oil shales (Roehler, 1961; Surdam and Wolfbauer, 1975).



EXPLANATION L: Late; M: Middle; E: Early; FM: Formation; B: Bed
 □ : Wasatch Formation ▨ : Green River Formation

Figure 3: Stratigraphic correlation diagram of lower Tertiary rocks in southwestern Wyoming (after Sullivan, 1980).

The Luman Tongue of the Green River Formation represents the initial deposits of Lake Gosuite. From the distinct facies present, it has been interpreted that Lake Gosuite evolved from a paludal-fluvial environment into an open-lacustrine system (Sklenar, 1982). It can be inferred that Lake Gosuite represented a shallow, fresh-water lake during the deposition of the Luman Tongue, because numerous streams fed the lake and evaporites are not present (Sklenar, 1982). Younger units of the Green River Formation contain abundant saline minerals (Snoke, 1997) and differ from the initial freshwater deposits of the Luman.

Eocene Climate

Abundant paleotropical floral taxa present during the Early Eocene in this part of North America indicate a moist subtropical climate (Leopold and MacGinitie, 1972) with extensive forests and abundant, large, perennial streams (Prichinello, 1971; Bown and Kraus, 1981; Sklenar and Andersen, 1985; Kirshbaum and others, 1994). Within the Washakie basin the paleoclimate ranged from subhumid to humid; tropical to subtropical vegetation grew on the alluvial plain around Lake Gosuite, which also supported a diverse gastropod fauna, crocodiles, turtles and various small mammals (Sklenar and Andersen, 1985).

Lower Eocene rocks display small floral differences throughout much of the area and suggest that the upland areas probably were areas of low relief. This low relief probably allowed consistent climatic conditions over a large geographic area (Leopold and MacGinitie, 1972).

Structural History

The present geomorphology of Wyoming owes many of its features to the Laramide orogeny. The Laramide orogeny reflects crustal strain probably caused by shear between the continental lithosphere and the subducting oceanic lithosphere (Bird, 1984) and also partly reflects the dramatic increase in the convergence rate between the North American and Pacific plates (Coney, 1978; Engebretson and others, 1984; Dickinson and others, 1988). From New Mexico to Montana, the Laramide orogeny resulted in the development of a belt of roughly arcuate, asymmetric, Precambrian-cored, thrust-faulted uplifts (Johnson, 1990; Snoke, 1997). Laramide activity in the Rocky Mountain region began in the Late Cretaceous and continued through the Eocene, with subsidence within the intermontane basins accompanying uplift of the Laramide ranges (Keefer, 1965; Sklenar, 1982; Dickinson and others, 1988).

The intermontane greater Green River structural basin (Green River, Bridger, Great Divide and Washakie basins) is bounded by numerous uplifts: the Wind River Mountains to the north, the Uinta Mountains to the south, and the Idaho-Wyoming fold and thrust belt to the west (Fig. 1). Located within this basin is an arched, Late Cretaceous and early Tertiary, north-trending anticline (Rock Springs uplift), flanks of which dip away from the axis at angles from about 1 or 2 degrees up to about 8 degrees (Bradley, 1964). From the present outcrop width and these inferred dips, Bradley (1964) estimated that the anticline had a structural relief of between 300 and 760 m. Kirschbaum and others (1994) put a maximum structural relief by the middle Paleocene of about 500 m based on the amount of Upper Cretaceous section that was removed at the

Cretaceous/Tertiary unconformity. Love and Christiansen (1985) showed the uplift to be bounded on the west by a thrust fault.

Most of the major structural features shown in Figure 1, including the Washakie basin, the Wind River, Uinta, and Big Horn mountains, and the Black Hills existed by the beginning of the Tertiary, although the Uinta and Wind River mountains were not as high as they later became (McGrew, 1971; Snoke, 1997). During the Paleocene epoch, subsidence created several lake-filled basins. Deposition continued without pause through the Eocene, resulting in deposition of the Fort Union and the Wasatch formations (Bradley, 1964).

Wyoming experienced widespread and intense deformation during the latest Paleocene and early Eocene. This structural deformation continued and became more complex during the Eocene, with further tectonic activity producing many folds and thrusts throughout Wyoming (McGrew, 1971). Substantial uplift and deep erosion during this time kept elevations low (Bradley, 1964; Leopold and MacGinitie, 1972).

Local Stratigraphy and Paleoenvironment

Roehler (1977) and Roehler and Valcarce (1978) mapped the Sand Butte Rim NW and Antelope Flats 7-1/2-minute quadrangles, respectively. On the Sand Butte Rim NW quadrangle, Roehler (1977) distinguished two limestone beds within the main body of the Wasatch Formation as stratigraphic marker beds "A" and "B". Although the "B" marker bed is the same on both quadrangles, Roehler and Valcarce (1978) mapped a different "A" marker bed, a limestone bed within the Wilkins Peak Member of the Green

River Formation on the Antelope Flats quadrangle. The “A” marker bed on the Sand Butte Rim NW quadrangle also correlates with the “T” limestone in the stratigraphic scheme of Savage and others (1972).

The composite stratigraphic section of the Sand Butte Rim NW map (Roehler, 1977) displays three limestone beds that are stratigraphically higher than the “B” marker bed. The composite stratigraphic section of the Antelope Flats map (Roehler and Valcarce, 1978) shows seven limestone beds in the Wasatch Formation that are stratigraphically higher than the “B” marker bed.

The main body of the Wasatch Formation comprises rocks that were deposited in an intermontane basin, mostly by streams upon floodplains (Roehler, 1979). Red beds are rare in this area, and any iron compounds present were reduced to form gray and green pigments, suggesting that the Eocene soils were moist or well saturated (Roehler, 1979). Fossils of mainly wood, seeds, leaves, spores and pollen collected from lower Eocene rocks in and adjacent to the Sand Butte Rim NW quadrangle indicate a pond and forest landscape with abundant hardwood trees (Roehler, 1979).

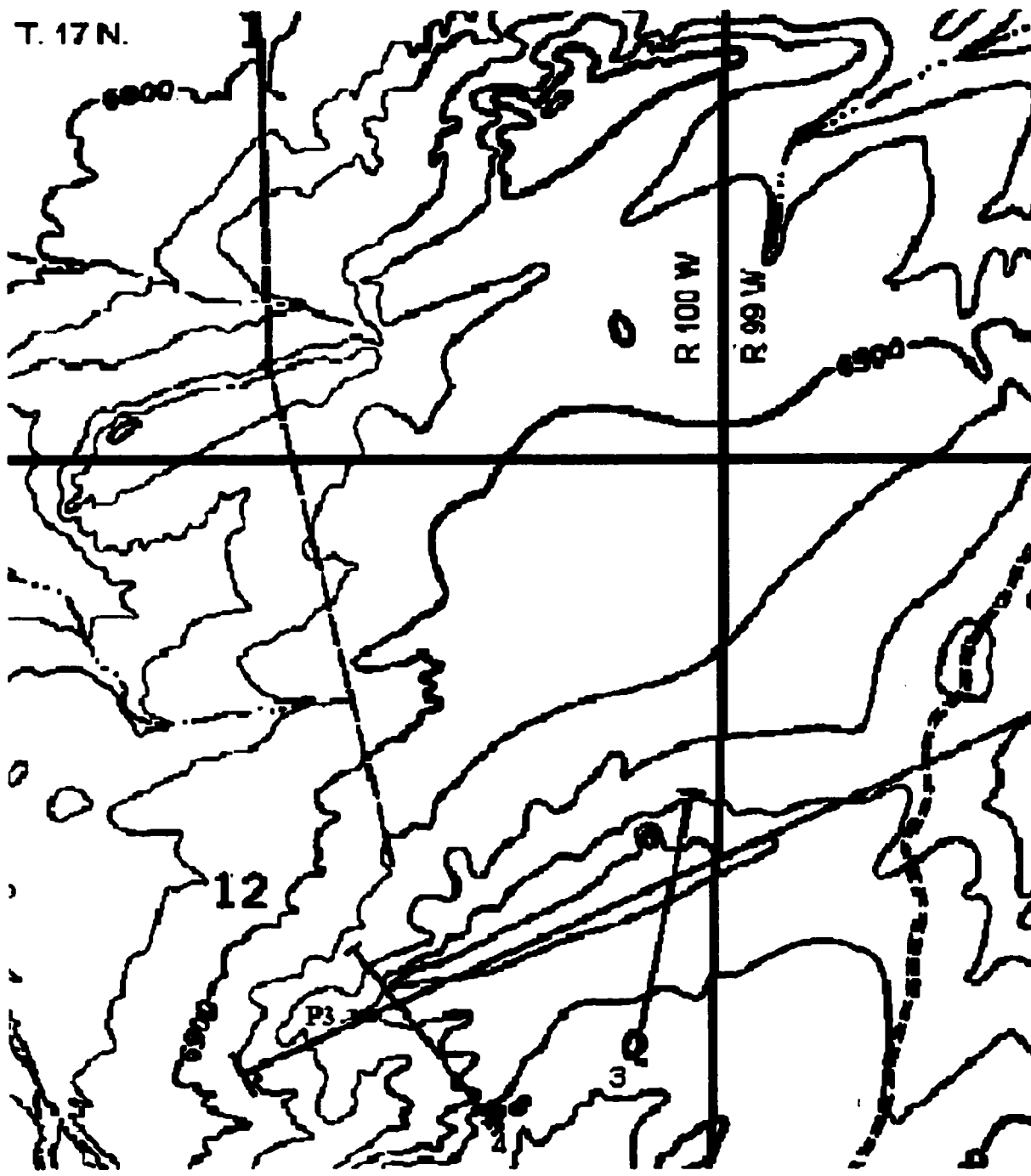
METHODS

Field Procedure

A field study of a portion of the main body of the Wasatch Formation along the southeastern flank of the Rock Springs uplift was accomplished during 2 weeks in October 1983. Fieldwork consisted of measuring stratigraphic sections and collecting samples from three limestone beds. The four sites for the measured sections were chosen so that the maximum stratigraphy at each end of the two sections of ridge exposed in the field area could be displayed.

Four stratigraphic sections were measured using a 1.7-m Jacob's staff with a Silva compass used as a clinometer. Rock colors were determined by using the rock-color chart of Goddard and others (1963). The locations of the stratigraphic sections are shown on Figure 4. The bottom of each stratigraphic section was placed at the break in slope at the base of the ridge in the field area (Fig. 5) below which the rocks are mostly covered. Section #1 was measured on the slope in the center foreground on Figure 5, and the slope in the background that projects toward the right is the location of stratigraphic section #2, which is also shown in Figure 6. Figure 7 shows the locations of sections #3 and #4 and the uppermost limestone at the top of the ridge, which was used to define the top of each section.

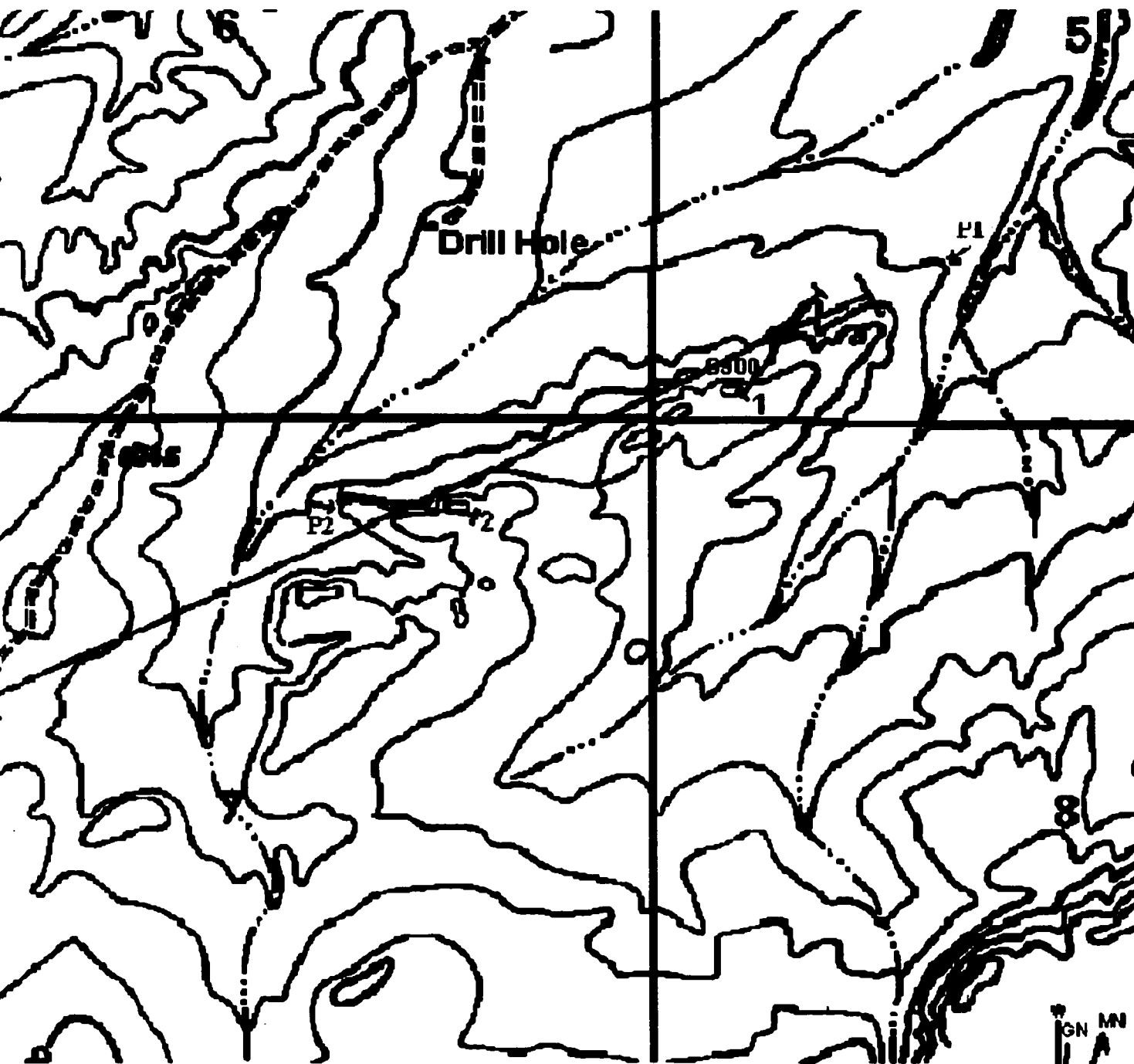
Forty-five limestone samples were collected from various localities in the field for analysis. These samples were later subjected to X-ray diffraction analysis, insoluble residue studies, and petrographic analysis. Distance measurements used for sample



EXPLANATION |——| Lines of measured sections. |——| E-W line

Scale: 0 ————— 1 Km

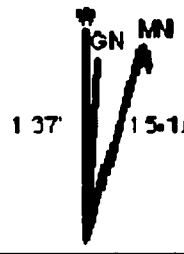
Figure 4. Topographic map compiled from Antelope Flats and Sand Butte Rim, 1



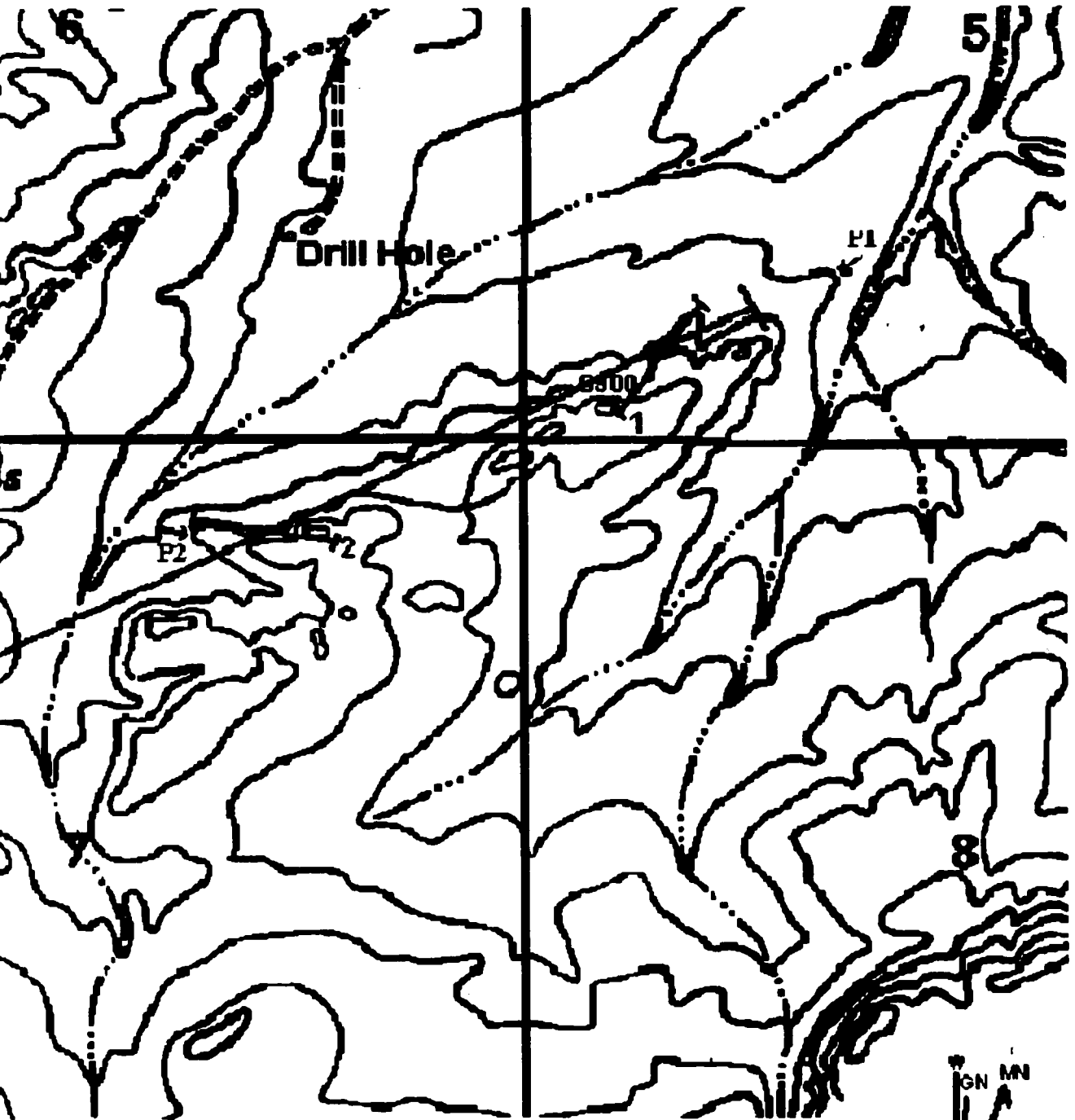
E-W line along which distance was measured for later figures.

1
Miles

Contour Interval 20 feet P's Picture locations

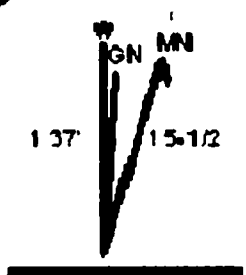


the Rim, NW 7-1/2" quadrangles showing measured sections #1 through #4.



which distance was measured for later figures.

les Contour Interval 20 feet P's Picture locations



1/2" quadrangles showing measured sections #1 through #4.



Figure 5. Photograph of measured section #1 (ridge in foreground) and section #2 (ridge in background, prominence facing right), showing ridge and break in slope towards base (view towards west). For location of photograph point, refer to P1 on Figure 4. Ridge in foreground is 10.5 m high from break in slope at base.

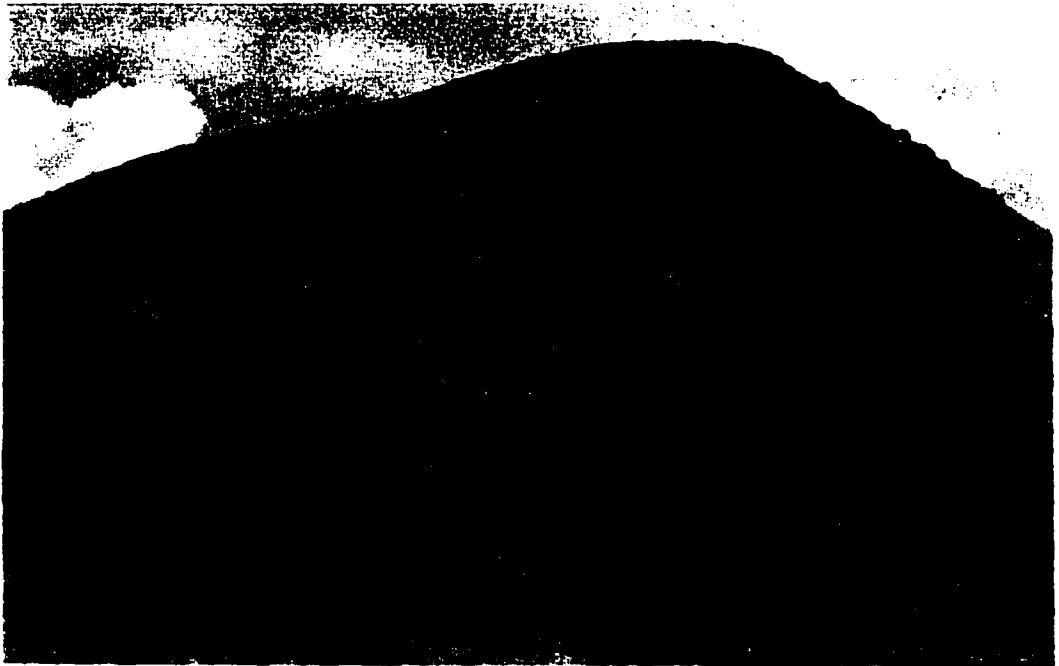


Figure 6. Photograph of measured section #2 in field area (view towards east). For location of photo point, refer to P2 on Figure 4. Ridge is 18 m high.



Figure 7. Photograph of measured sections #3, ridge on left, and #4, foreground on right (view towards east). For location of photo point, refer to P3 on Figure 4. Ridge is 18 m higher than break in slope at base to left.

locations on later figures were determined by measuring with a ruler directly from the topographic map and calculating distances from a point at the eastern edge of the field area and projected onto the east-west line pictured in Figure 4.

Laboratory Procedure

Samples of the three limestone beds were collected at the measured sections and areas between them (Figs. 4 and 8) and were analyzed in the laboratory. This laboratory work consisted of X-ray diffraction, insoluble residue and petrographic analysis. A number of rock fragments, representative of each sample, was ground up and sieved to minus 200 mesh for X-ray diffraction and insoluble residue analysis. A minimally weathered and intact portion of each sample was chosen for thin sectioning and petrographic analysis.

X-ray Diffraction

The samples were analyzed by X-ray diffraction to determine the carbonate mineralogy and to identify some of the non-carbonate minerals. A copper tube was used in a Norelco X-ray diffractometer that was set at 35 kilovolts and 15 milliamps. The samples were scanned from 20 to 42 degrees 2θ at a scanning speed of $2^\circ 2\theta/\text{minute}$, with a time constant of 1 second and a detector range set at 2500 counts per second. All of the samples were analyzed with the same instrumental conditions.

Within the range of 20 to 42 degrees 2θ , numerous mineral peaks can be discerned. The six main minerals that are the focus of this study are calcite, dolomite,

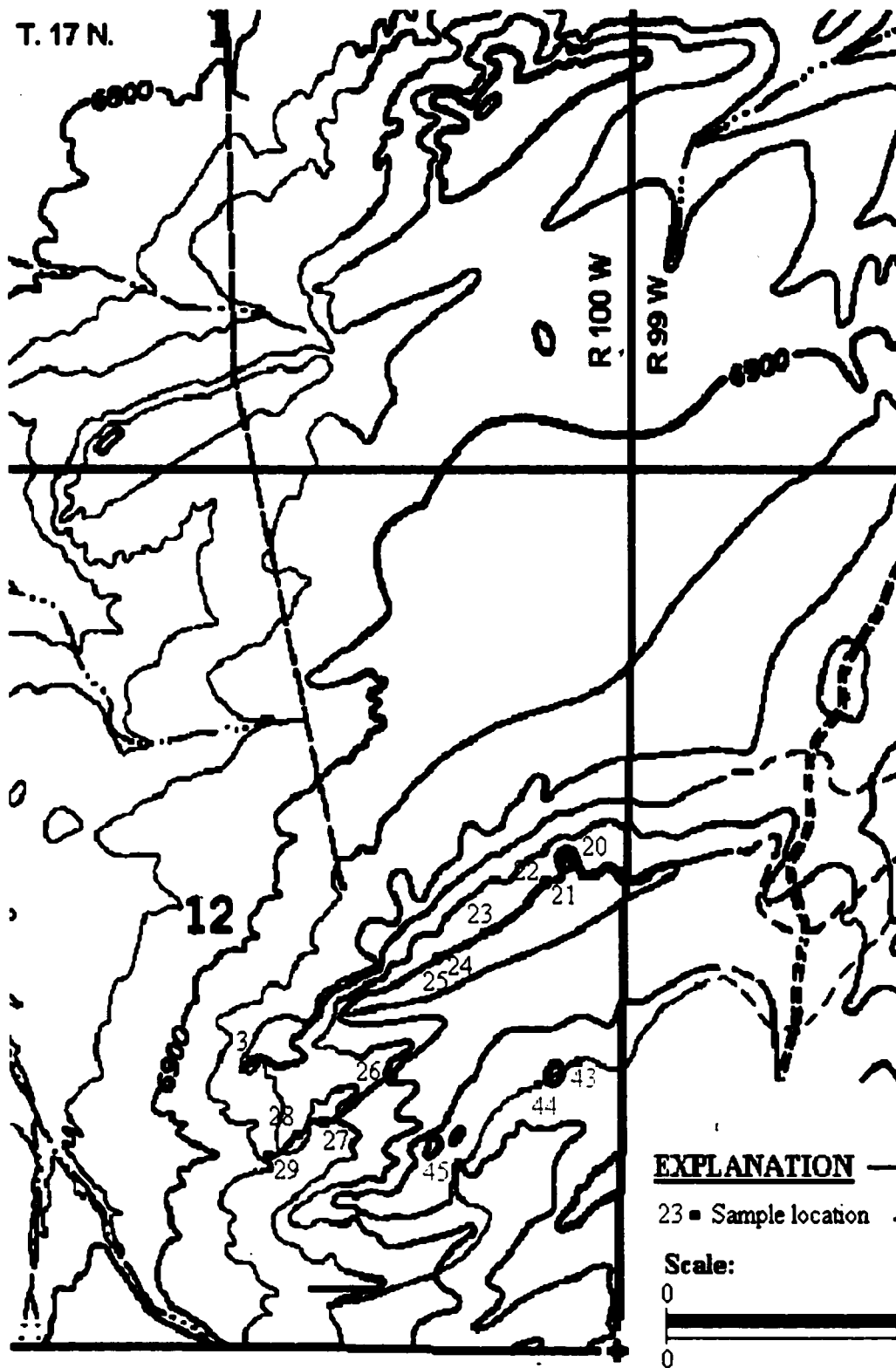
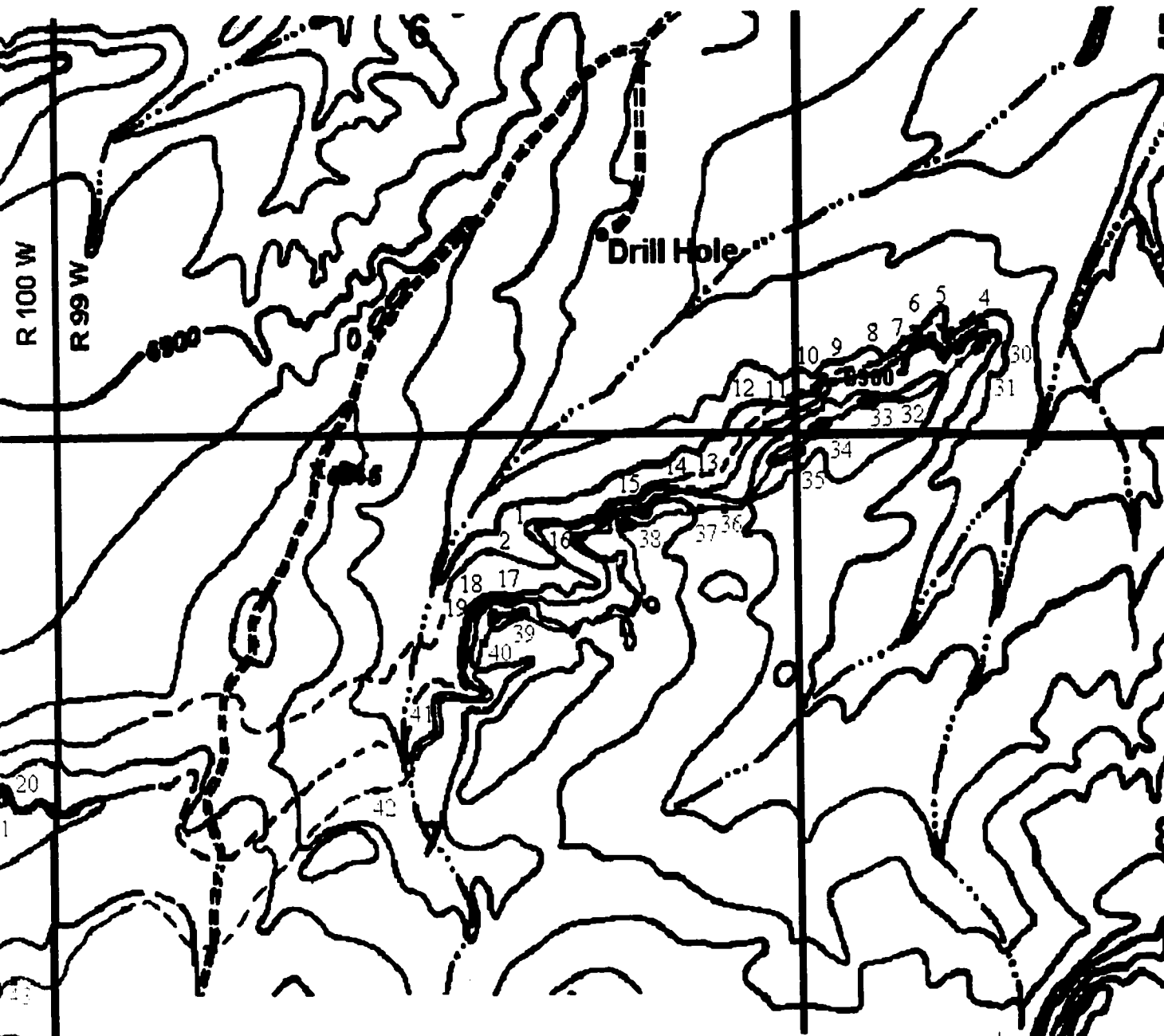


Figure 8. Topographic map compiled from Antelope flats and Sand Butte Rim, N.



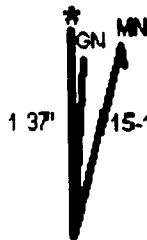
EXPLANATION

— Bed #1 — Bed #2 — Bed #3

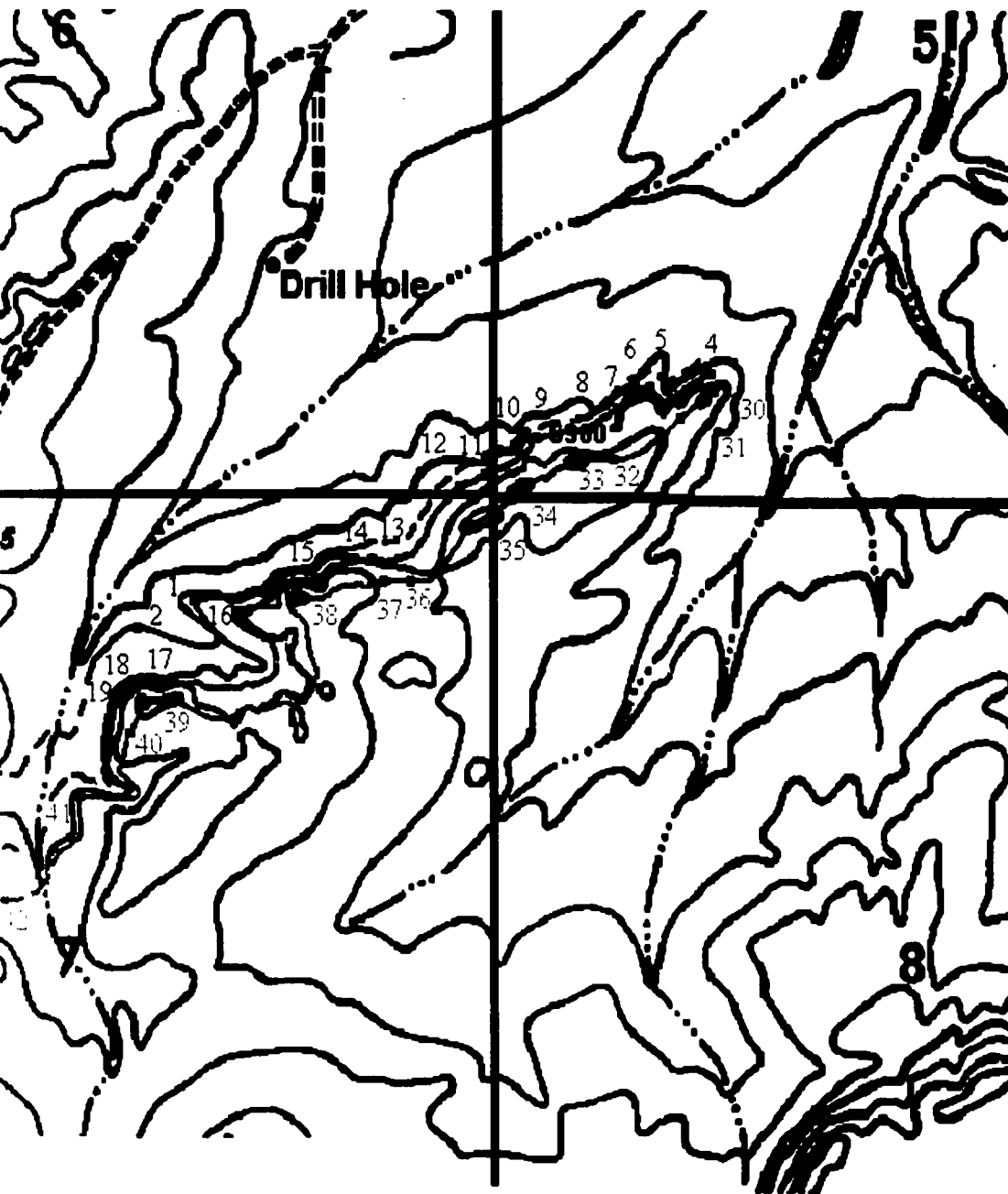
23 ■ Sample location — Trace of bedding (dashed where covered or approximate)

Scale:

Contour Interval 20 feet



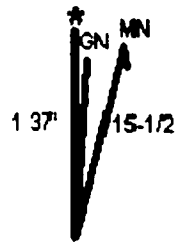
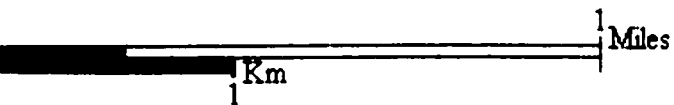
telope flats and Sand Butte Rim, NW 7-1/2" quadrangles showing locations of samples and bedding in field area.



#1 — Bed #2 — Bed #3

Trace of bedding (dashed where covered or approximate)

Contour Interval 20 feet



2" quadrangles showing locations of samples and bedding in field area.

quartz and the feldspars albite, microcline and orthoclase. The expected 2θ positions and peak height intensities for these minerals were taken from the Mineral Powder Diffraction Data Book (1980) and Mineral Powder Diffraction Search Manual (1974).

The positions and intensities of all the significant peaks for each sample were noted. Each peak was then identified and labeled as to which mineral component it represented. The relative abundance of minerals was gauged against the calcite peak. Because calcite is the predominant mineral in all of the samples, the instrumental conditions were set so that the calcite peak was approximately 100 out of 100 on each chart-recording strip. Other minerals were determined to be abundant, common or present in trace amounts depending on the height of their maximum peaks. If the maximum peak intensity was 25 or more, then that mineral was considered abundant. Minerals with peak height values ranging from 10 to 24 were deemed to be common, and minerals with peaks of 9 or less were considered to be present in trace amounts. The X-ray data were cross-referenced with the insoluble residue data, and the relative amount of residue was used to determine X-ray values delimiting each range (abundant, common, trace).

Variations in sample preparation and adjustments of the X-ray diffractometer can influence the accuracy and reproducibility of intensity measurements. Variables connected with sample preparation include grinding, packing within the sample holder and preferred orientation. Important instrumental variables include scanning speed, time constant, range setting and miscellaneous others. These variations were minimized to the extent possible with these samples. Other differences in peak heights can be explained

by the interference effect that certain minerals, such as quartz, can have on calcite and dolomite (e.g., Lumsden, 1979). Peak intensities for carbonate and silicate minerals are therefore not always in direct proportion to relative abundance.

Insoluble Residue

An insoluble residue analysis was done to determine what portion of each limestone sample consists of non-carbonate minerals. This analysis was also used to cross-reference the data from the X-ray and petrographic analyses. The insoluble residue analysis was accomplished by dissolving approximately 5-g samples of crushed limestone in 6 N hydrochloric acid. The remaining solution was then dried on a hot plate to drive off all the acid. A 1 N hydrochloric acid solution was then added to turn the dried residue back into solution. This solution was then vacuum filtered through a plain white 47-mm-diameter membrane filter with a pore size of 0.45 μm . The filtrate was then oven dried at 40° C for 24 hours. The dried samples were then weighed to determine their final residue weight. Three limestone samples were run from each sampling site to determine how much variability there might be in the residue values at that site.

Petrography

Point counts of petrographic thin sections of all forty-five carbonate samples were done. In each sample, 300 randomly selected points were counted. Items counted consisted of fossils (ostracods, gastropods and pelecypods), pellets, intraclasts, coated

**grains, matrix, cement, non-carbonate grains (quartz, feldspar, apatite, rock fragments)
and pore space. Unidentifiable materials were counted as other.**

RESULTS

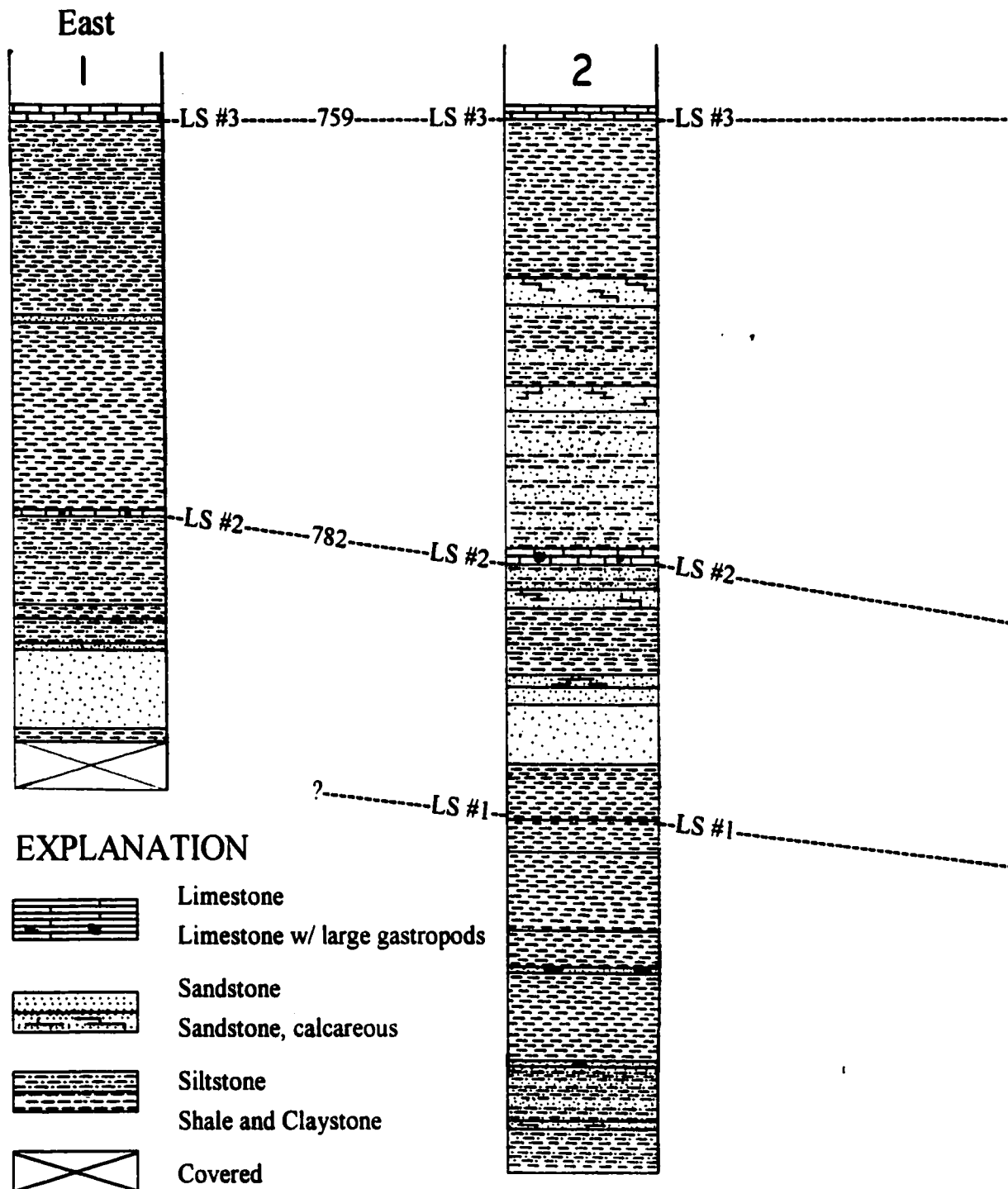
Stratigraphy


Three distinct limestone beds are prominent within the field area. Herein, these beds will be designated, from oldest to youngest, limestone #1, limestone #2 and limestone #3. Limestone bed #3 correlates with the "T" limestone described by Savage and others (1972) and the "A" marker bed of Roehler (1977). A detailed description of these limestones and other rocks at the four measured sections is provided in Appendix A and the sections are illustrated in Figure 9. Samples were collected both along the lines of the sections and from localities between the sections (Figs. 4 and 8).

Limestone #1

Limestone #1 is the lowest stratigraphic unit included in this study. This bed is continuous from measured stratigraphic section #4 to #2, but is covered to the east (section #1).

This bed is very distinctive in the field area. It is typically dark to light gray in color with very thin, black, fossiliferous layers. The limestone weathers from pale yellow to pale olive. This bed thickens westward from 3 cm at stratigraphic section #2 to 8 cm at stratigraphic section #3, but then decreases in thickness to 2 cm at section #4. The predominant fossils throughout this bed are pelecypods. The gastropods are in the range of millimeters to centimeters in size. Shale occurs below and above this bed at each of the measured sections. Three samples of limestone #1 were collected for analysis.

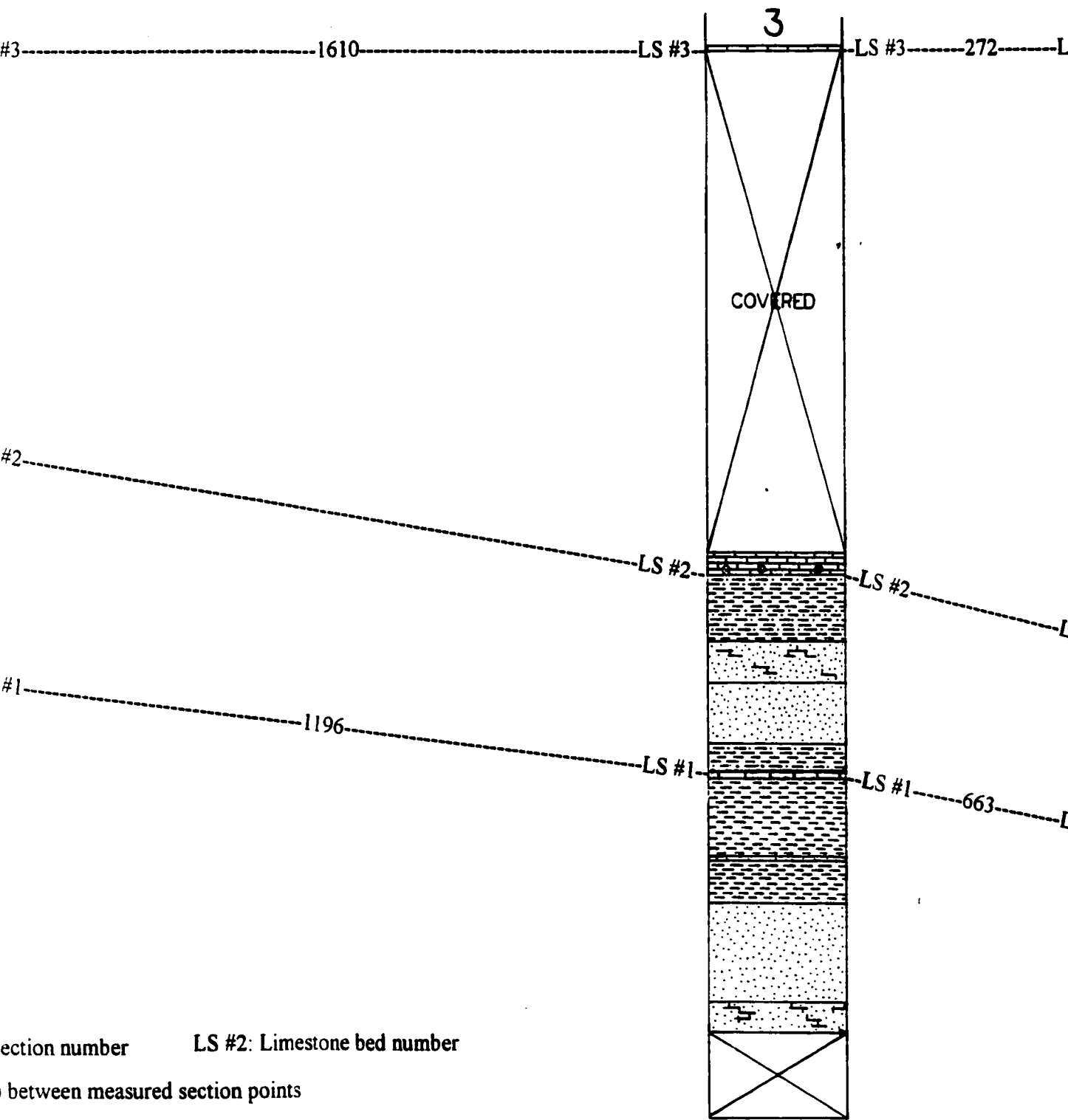


Vertical Scale:  1 meter

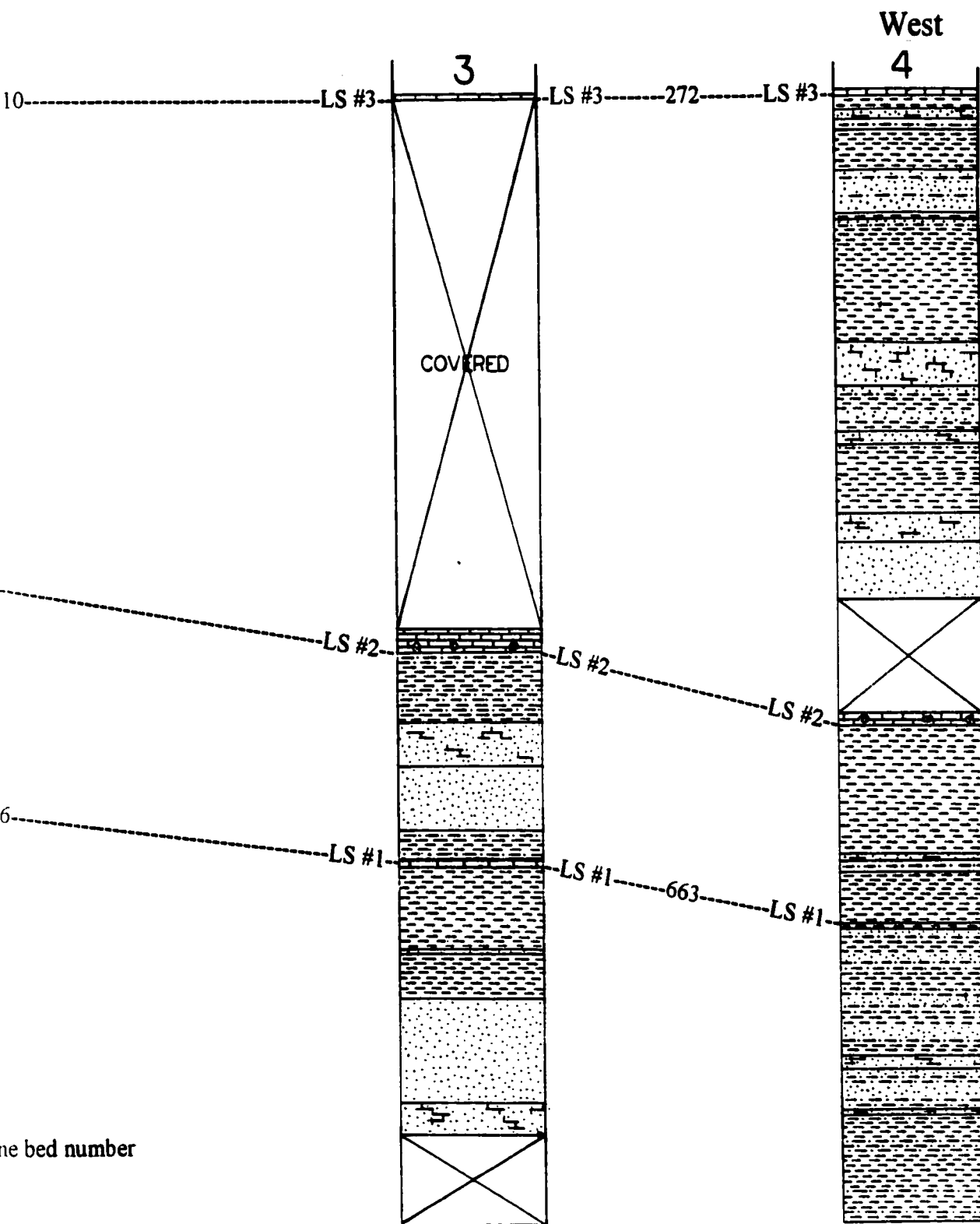
3: Measured section number LS #2: L

----- 123 ----- Bed correlation lines and distance (in meters) between measured section po

Figure 9: Measured sections #1 through #4, showing stratigraphic relationships. Locations of m



Section number LS #2: Limestone bed number
 between measured section points
 relationships. Locations of measured sections shown on Figure 4.



sections shown on Figure 4.

At stratigraphic section #2, this limestone is medium-dark to dark gray and pale yellow at the bottom, grading to light gray towards the top. Weathering produces pale yellow, light yellowish gray and pale olive colors. There is one especially closely packed layer of fragmented fossils at the bottom of this bed. The underlying and overlying shales are light gray in color.

This limestone at section #3 ranges in color from greenish gray to medium gray and weathers pale yellow to pale olive. The bed is mostly massive except for the 1- to 2-cm-thick, highly fossiliferous layers. The underlying shale is dark gray. The overlying siltstone and shale is dark gray at its base, but coarsens upward into light-gray, very fine-grained sandstone over a 62 cm thickness.

At section #4, limestone #1 is light gray to very light gray in color with medium-dark-gray fossiliferous layers and weathers pale yellow to light dusky yellow. The top half of the bed becomes very light gray. The predominantly massive nature is similar to that at measured section #3. The layering that is present at section #4 is less distinct than that observed at section #3. The pelecypods are both intact and partially fragmented, and they are only a few millimeters in size. The underlying shale is dark gray. The overlying shale alternates between light and dark gray layers.

Limestone #2

The middle carbonate unit in this study is limestone #2. The color of this bed is quite variable, ranging from very pale grayish orange and pale grayish orange to yellowish gray, light yellowish gray and pale pinkish gray. The limestone typically

weathers to pale yellow, yellow and yellowish gray. This bed is massive throughout the field area. The bed thickens from 8 cm at section #1 to at least 40 cm at section #3, and then thins to 18 cm at section #4. The distinctive feature of this bed is the presence of numerous, large (centimeter-sized) gastropods. This bed is well exposed in the field area, and twenty-six samples were collected for analysis. Because it was difficult to find a fresh sample at each site, sampling was not always consistently done at the same stratigraphic level within the bed along the strike of the bed.

At section #1, the limestone is very pale grayish orange to pale grayish orange, very pale orange and pale pinkish gray, weathering pale yellow, yellow and yellowish gray. This bed is massive and gastropod rich. The underlying bed is olive-gray siltstone and claystone. Dark-gray shale and claystone with minor silt overlie this limestone. The siltstone is flaky and the claystone is crumbly, becoming more indurated towards the limestone contact. The contact of the lower bed with the limestone is not very distinct.

At section #2, this limestone is yellowish gray to light yellowish gray and pale grayish orange to very pale grayish orange, weathering yellow to yellowish gray and pale yellow. This bed is massive and fractured. Underlying this limestone is gray, very fine-grained sandstone that grades into a clay-rich siltstone at the limestone contact. Above this limestone is a pale-brown to yellow siltstone and very fine-grained sandstone. The sandstone layers have thin intervals of cross-laminations. Rip-up clasts and flame structures are also present.

At section #3, the limestone is light gray to pale yellow and very pale grayish orange, weathering pale yellow. The bed is massive and appears crystalline. Large

gastropods are present at the base of the bed, but they are not as numerous as at sections #1 and #2. The upper portion of the bed contains small, millimeter-size gastropods. Underlying this bed is dark-gray siltstone and shale that darkens upwards to very dark gray with a 10-cm-thick, light-brown siltstone layer at the limestone contact. Above this limestone is a thick covered section.

At section #4, the limestone is pale to very pale grayish orange and very pale yellowish brown, weathering grayish brown to light brownish gray. The bed is massive and fractured, but here small to large gastropods are abundant. Below this limestone is dark-gray shale that lightens in color to gray towards the base of the shale. Above this limestone is a covered section.

Limestone #3

Limestone #3 is the bed that forms the ridge in the field area. The true thickness of this bed is hard to determine because it is exposed along the top of the ridge and the overlying rocks are covered, but exposed sections range from 10 to 30 cm thick. The color ranges from light gray and very pale orange, to very pale grayish orange, pale grayish orange and pale yellowish brown. Similar to limestone #2, this bed is massive.

Gastropods are common and typically 1 mm in size, compared to the centimeter-size gastropods in bed #2. Typical weathering colors are very pale grayish orange, light grayish orange pink, pale yellow and yellowish brown. Because this limestone is highly fractured and the outcrops are poor, only sixteen samples were obtained for analysis.

At section #1, the limestone is light gray, very pale orange and pale grayish orange, weathering pale yellow, light grayish orange pink and yellowish brown. There are minor amounts of large, intact, gastropods with some minor fossil fragments. The lower contact is irregular. The bed underlying this limestone is composed of light-gray siltstone and claystone.

The limestone at section #2 is pale yellowish brown in color and weathers light gray to yellowish brown. Here the rock has a crystalline appearance, similar to some of the other sites in the field area. Fossils are sparse and are predominantly 0.5-mm gastropods. The bed directly below this is a yellowish-brown to dark-gray shale and siltstone that is highly weathered and crumbly.

At section #3, this limestone is mottled yellow, weathering reddish yellow. The bed is massive with rare light-gray fossil fragments. Below this limestone is a thick covered section that separates bed #3 from bed #2.

At section #4, this limestone is very pale grayish orange and weathers gray. This bed also has a crystalline appearance and has rare fossils. Below this limestone is shale that is mostly covered.

Laboratory Analysis

All of the data from X-ray, insoluble residue and petrographic analyses were assembled into one compilation (Table 1). This was done so that comparisons could be made between the different sets of data. All of the data are broken down by bed starting with bed #1 (oldest) and ending with bed #3 (youngest). Point-count percentages for total fossils, matrix plus cement, total carbonate and non-carbonate grains were

TABLE I. MASTER TABLE OF X-RAY, RESIDUE AND POINT COUNT DATA

Lime- stone bed	Sample number	X-ray data ¹				Residue				Point count data				Total of Qtz, Fld and Otr
		Ca ²	Dol ²	Qtz ²	Fld ²	Res ² %	Car ² %	Qtz ² %	Fld ² %	Otr ² %	Fld ² %	Otr ² %		
# 1	1	XXX		X	X	3.81	98.3	0.0	0.3			1.4	1.7	
	2	XXX				0.89	100.0	0.0	0.0			0.0	0.0	
	3	XXX				1.97	99.5	0.0	0.0			0.5	0.5	
	4	XXX	X	X	X	5.67	93.3	4.4	1.7			0.6	6.7	
	5	XXX	X	X		5.30	98.3	0.3	0.3			1.1	1.7	
	6	XXX	X	X		4.90	98.0	1.0	0.7			0.3	2.0	
	7	XXX	X	X		2.97	99.7	0.3	0.0			0.0	0.3	
	8	XXX	X	X		10.00	99.3	0.0	0.7			0.0	0.7	
	9	XXX	X	XXX	X	31.16	91.0	8.0	1.0			0.0	9.0	
	10	XXX	X	XXX	X	29.84	89.3	6.7	1.7			2.3	10.7	
	11	XXX	X	X	X	4.96	98.0	0.0	1.3			0.7	2.0	
# 2	12	XXX	X	XXX	X	41.47	69.9	21.4	7.7			1.0	30.1	
	13	XXX		X	X	5.21	100.0	0.0	0.0			0.0	0.0	
	14	XXX	X	XX	X	20.66	96.9	2.4	0.4			0.3	3.1	
	15	XXX	X	XX	X	12.61	96.6	2.7	0.0			0.7	3.4	
	16	XXX	X	XXX	X	32.81	81.3	15.1	3.0			0.6	18.7	
	17	XXX	X	XX	X	23.01	90.6	7.7	1.0			0.7	9.4	
	18	XXX	X	XX	X	10.25	97.0	1.0	0.0			2.0	3.0	
	19	XXX	X	XX	X	20.80	83.6	12.1	3.7			0.6	16.4	
	20	XXX	X	X		6.08	96.0	2.7	1.0			0.3	4.0	
	21	XXX	X	X	X	5.66	97.3	2.3	0.0			0.4	2.7	
	22	XXX	X	X	X	2.96	100.0	0.0	0.0			0.0	0.0	
	23	XXX	X	X	X	3.96	97.0	3.0	0.0			0.0	3.0	

EXPLANATION: XXX: Abundant XX: Common X: Trace

1: Blank spaces do not denote 0 values, rather they denote areas of non-detection or unreliability.

2: Cal: Calcite, Dol: Dolomite, Qtz: Quartz, Fld: Feldspar, Res: Residue, Car: Carbonate, Otr: Other

TABLE 1. MASTER TABLE OF X-RAY, RESIDUE AND POINT COUNT DATA (continued)

Lime- stone bed	Sample number	X-ray data ¹				Residue				Point count data				Total of Qtz, Fld and Otr
		Cal ²	Dol ²	Qtz ²	Fld ²	Res ² %	Car ² %	Qtz ² %	Fld ² %	Otr ² %	Fld ² %	Otr ² %		
	24	XXX		X		4.06	98.0	1.0	0.0	1.0	0.0	1.0	2.0	
	25	XXX	X	XXX	X	31.42	86.0	11.3	2.0	0.7	2.0	0.7	14.0	
	26	XXX		X	X	6.51	98.7	1.3	0.0	0.0	0.0	0.0	1.3	
	27	XXX		X		24.91	97.7	0.7	1.0	0.3	1.0	0.3	2.0	
# 2	28	XXX		X	X	6.63	97.3	1.7	0.0	1.0	0.0	1.0	2.7	
	29	XXX		X		6.46	99.3	0.7	0.0	0.0	0.0	0.0	0.7	
	30	XXX		X	X	5.26	98.7	0.0	0.0	1.3	0.0	1.3	1.3	
	31	XXX		X	X	3.83	99.0	0.0	0.7	0.3	0.7	0.3	1.0	
	32	XXX		X		1.48	100.0	0.0	0.0	0.0	0.0	0.0	0.0	
	33	XXX		X	X	1.79	97.7	0.0	0.0	2.3	0.0	2.3	2.3	
	34	XXX		X	X	6.09	97.0	1.7	1.0	0.3	1.0	0.3	3.0	
	35	XXX		X	X	1.05	99.0	0.0	0.7	0.3	0.7	0.3	1.0	
	36	XXX		X	X	0.63	99.7	0.0	0.3	0.0	0.3	0.0	0.3	
# 3	37	XXX		X		1.67	87.6	7.2	4.8	0.4	4.8	0.4	12.4	
	38	XXX			X	1.29	99.3	0.4	0.3	0.0	0.3	0.0	0.7	
	39	XXX		X		0.59	99.3	0.0	0.4	0.3	0.4	0.3	0.7	
	40	XXX		X		2.51	100.0	0.0	0.0	0.0	0.0	0.0	0.0	
	41	XXX		X		1.55	100.0	0.0	0.0	0.0	0.0	0.0	0.0	
	42	XXX		X		3.02	99.3	0.7	0.0	0.0	0.0	0.0	0.7	
	43	XXX	XXX	X		4.07	99.7	0.0	0.0	0.3	0.0	0.3	0.3	
	44	XXX	XXX	X		2.01	98.3	0.7	0.3	0.7	0.3	0.7	1.7	
	45	XXX	X	X		2.03	99.7	0.3	0.0	0.0	0.0	0.0	0.3	

EXPLANATION: XXX: Abundant XX: Common X: Trace

1: Blank spaces do not denote 0 values, rather they denote areas of non-detection or unreliability.

2: Cal: Calcite, Dol: Dolomite, Qtz: Quartz, Fld: Feldspar, Res: Residue, Car: Carbonate, Otr: Other

calculated exclusive of pore space. Feldspar percentages were calculated inclusive of plagioclase and microcline (orthoclase was not observed). Apatite, rock fragments and unidentifiable grains were grouped, and the total of these point-counted grains was used to determine percentages for the “other” category.

X-ray Diffraction

The limestone samples were analyzed and the results are shown in Appendix B and Table 1. Appendix B lists the height of the maximum peak for each of the minerals detected in each sample. As can be seen from Table 1, all of the samples contain calcite as an abundant constituent. Although the X-ray machine settings were set to make the calcite peak heights as close to 100 as possible, Appendix B shows that calcite peak values range from a low of 57 to a high of 105.

Calcite is abundant in all samples. A total of eleven samples from different locations in bed #2 and #3 also contain dolomite. Dolomite, however, is an abundant component in only two of the samples, from limestone bed #3 located at stratigraphic section #3. Trace amounts of dolomite occur in nine other samples from beds 2 and 3 that are scattered throughout the field area. Quartz also is present in at least trace amounts in a majority of the limestone samples, and it is an abundant component in five of the samples from bed #2. Feldspars were detected in twenty of the limestone samples but only as a trace constituent.

Insoluble Residue

The averaged results of the residue analysis are given in Appendix C and Table 1. As can be seen from Appendix C, the results for all the beds are quite variable. All of the samples with more than 10% insoluble residue are from bed #2.

The 3 samples from bed #1 have average residues ranging from 0.89% to 3.81%. The average residue value for this bed is 2.22%, and the standard deviation as percent of average ranges from 23% to 67%.

Bed #2, which has the largest number of samples, also has the largest range of residue values. The lowest residue amount in this bed is 2.96%, and the highest is 41.5%. The average residue value for bed #2 is 13.5% and nine of the twenty-six samples have values of 20% or higher. The standard deviation as percent of average for bed #2 ranges from 1.1% to 41%. Seven of these samples are above 15% and only three of these seven samples exceed 20%.

The range of values from bed #3 is similar to that of Bed #1, with a low of 0.59% and a high of 6.09%. The average residue value for this bed is 2.99%. The standard deviation as percent of average for bed #3 ranges from 7.8% to 55%.

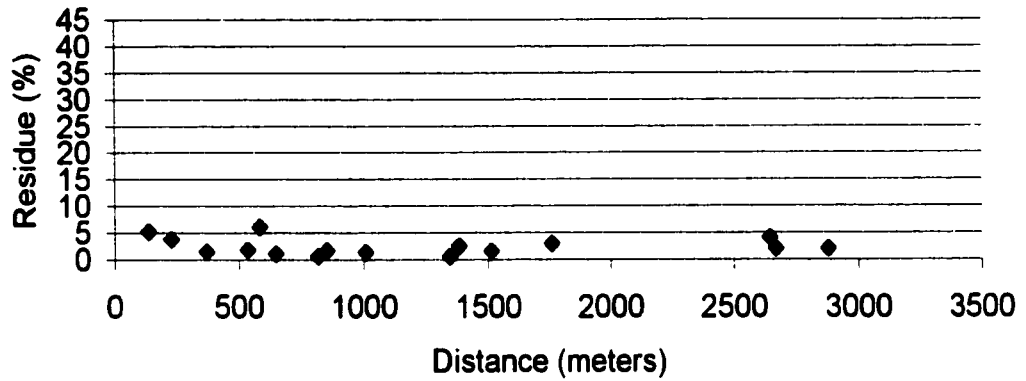
The residue data were plotted relative to distance, measured from the east edge of the field area (Fig. 10). Residue values range from 0.59% to 41.5%, over a distance of about 3190 meters.

Figure 10a shows amount of residue versus distance for bed #1. The largest residue value is from the easternmost sample, although the next sample to the west has

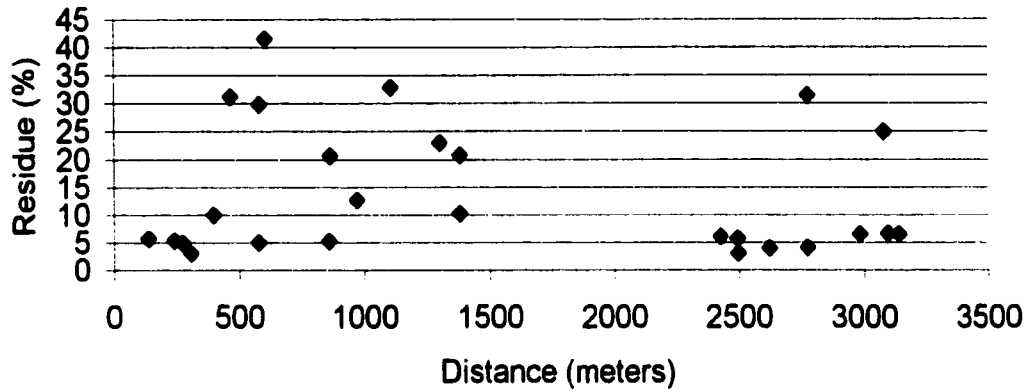
W

E

c) Bed #3



b) Bed #2



a) Bed #1

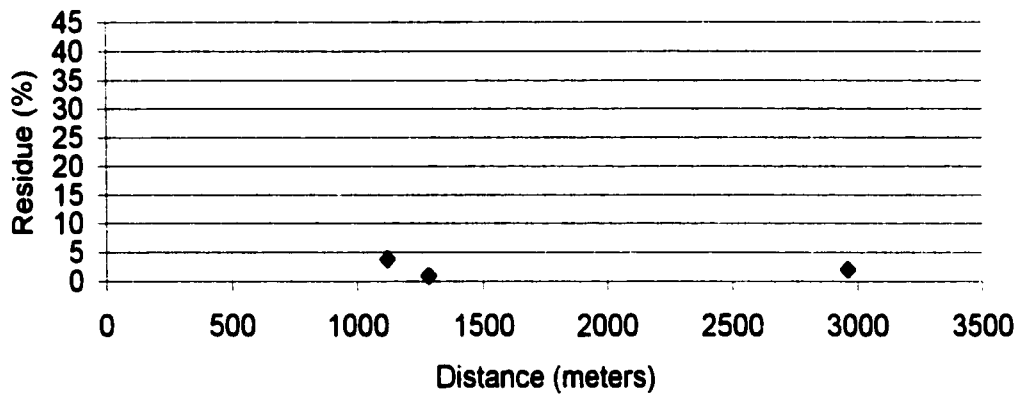


Figure 10: Residue versus distance from eastern edge of the field area for limestone beds #1 through #3 (see Fig. 4 for line of projection).

the lowest residue value for this bed, and the westernmost sample has a value intermediate between the first two.

Figure 10b shows the residue value versus distance in bed #2. The residue values fall within four specific groups: 3 – 7%, 10 – 13%, 20 – 25% and 29 – 42%. For discussion, these ranges will be designated low, medium, high and very high, respectively.

The residue values for bed #2 are quite variable over the length of the bed. The values are low near the eastern end of the field area, but become very high just a few hundred meters to the west. Very high and low residue values occur in adjacent samples throughout the eastern and central portions of this bed. Residue values are highest in sample #12. Sample #19 at the eastern edge of the large covered interval also has a high residue value. West of the covered section, eight of the ten samples have low residue values. Sample #25 has a very high value and #27 has a high value.

Overall, there is no clear trend for the residue values over the length of the bed from east to west. The only group of samples that is consistently medium to very high is samples #14 through #19, and most of the very high values are in the east. No other obvious patterns of residue amounts versus distance are evident for this bed.

Figure 10c shows residue versus distance for bed #3. Only five of the sixteen samples have residue values that exceed 3%. The samples with more than 3% residue are scattered from samples #30 to #43.

All of the very high residue contents occur in bed #2 (Fig. 10), although this bed also has a larger range of values than beds #1 and #3. Because of the occurrence of high

residue values in bed #2, this property could be useful in correlating this bed across large covered intervals.

Petrography

Point-count data are shown in Appendix D and summarized in Table 1. Thirty-five of these samples can be classified as biomicrites, five are sandy biomicrites, four are classified as fossiliferous micrites and one is a sandy fossiliferous micrite (Folk, 1980). Samples #9, #20, #21, #25 and #29, all of which are from bed #2, are fossiliferous micrites. If classified using Dunham's (1962) classification scheme, forty samples are classified as wackestone and five samples are classified as mudstone. The five mudstones are also samples #9, #20, #21, # 25 and #29. Six of the forty-five samples contain more than 10% terrigenous sand and silt visible petrographically.

A representative photomicrograph was taken of each bed. Figure 11 is an example of a pelecypod-rich biomicrite from bed #1. Figure 12 shows a very fine-grained sandy biomicrite from bed #2 containing both gastropods and pelecypods. Figure 13 is a biomicrite in bed #3 that shows both small and large gastropod fossils. Figure 14 shows an intact *Biomphalaria* (gastropod), surrounded by pelecypod fragments and abundant micrite, from a biomicrite from bed #2.

Several combinations of the 9 components (ostracods, gastropods, pelecypods, pellets, intraclasts, coated grains, matrix, cement and non-carbonate grains) were analyzed for useful groupings or significant trends. Five of these trends will be described in detail here.

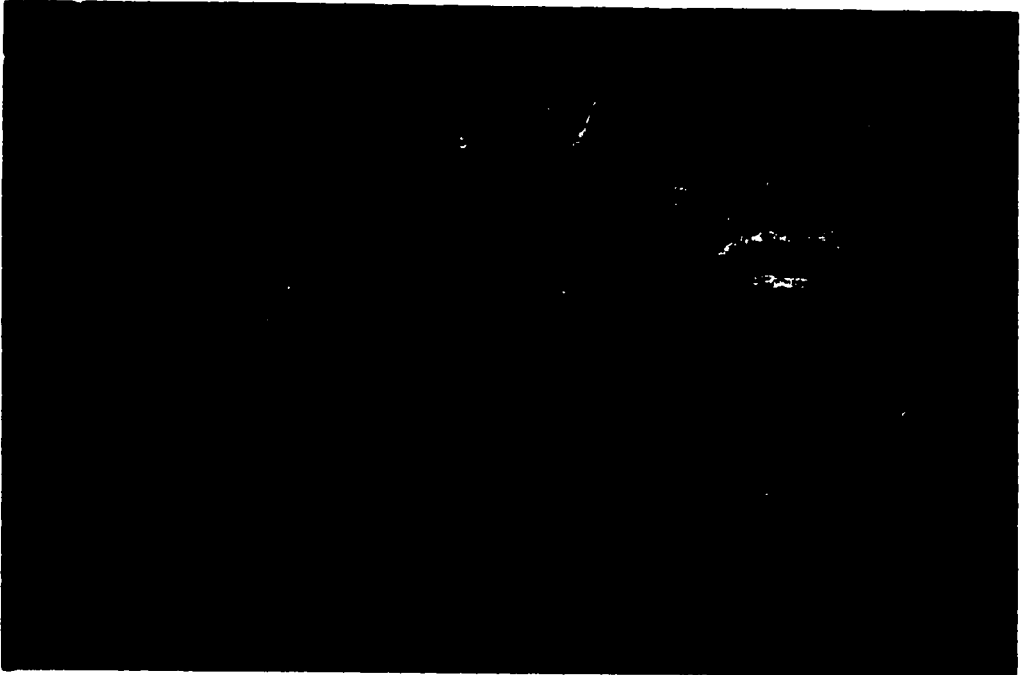


Figure 11. Photomicrograph of biomicrite in bed #1. Field of view is 5.6 mm across.



Figure 12. Photomicrograph of biomicrite in bed #2. Field of view is 5.6 mm across.

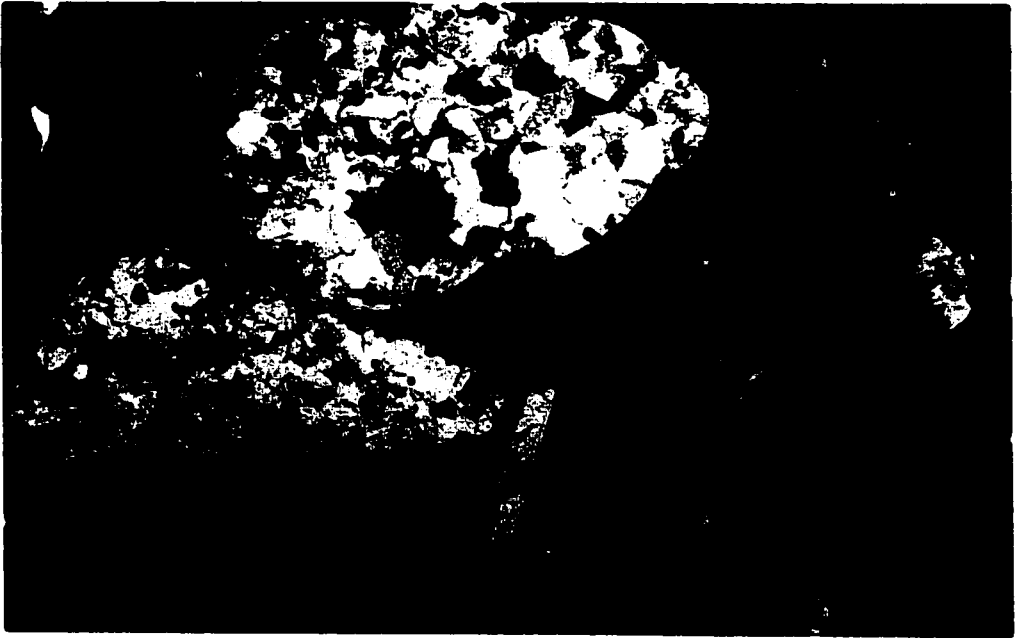


Figure 13. Photomicrograph of biomicrite in bed #3. Field of view is 5.6 mm across.



Figure 14. Photomicrograph of *Biomphalaria* in biomicrite from bed #2. Field of view is 5.6 mm across.

Figure 15 shows total fossils versus matrix for all three of the limestone beds. Fossils range from 0.3% to 36%. Matrix content ranges from a low of 59% to a maximum of 91%. Because fossils and matrix are the most abundant components present, their total commonly approaches 100%, but the addition of other components causes points to fall below this 100% line.

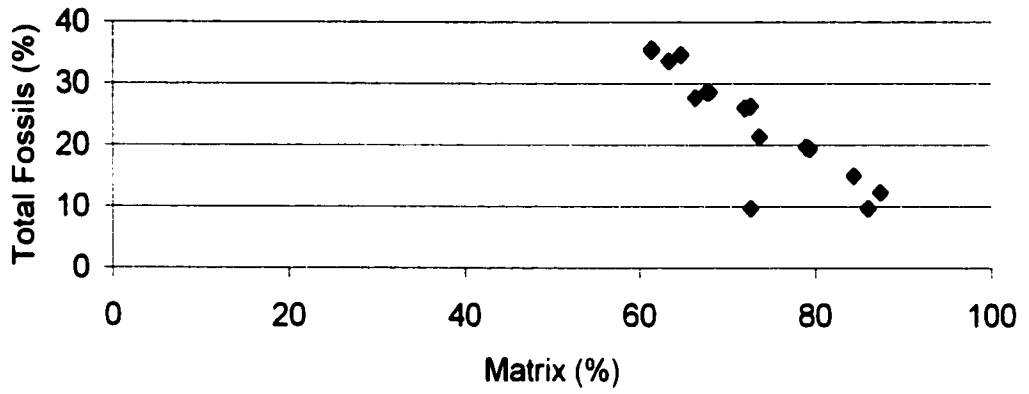
In bed #1, total fossils range from 19% to 28%, with an average of 24%, and matrix ranges from 65% to 81%, with an average of 72% (Fig 15a). Bed #1 is very low in non-carbonate grains, and fossils and matrix make up at least 96% of the components in this bed, so deviation of points from the 100% line is minimized.

In bed #2, total fossils range from 0.3% to 34%, with an average of 16%, and matrix ranges from 59% to 91%, with an average of 75% (Fig. 15b). Bed #2 has the same overall trend as bed #1, but because more terrigenous materials are present, divergence from the fossil-matrix line is noticeable (Fig. 15b). There is a large scatter of fossil percentages at lower matrix percentages, and less scatter when matrix percentages are above 85%. Unlike bed #1, in which non-carbonate grains do not exceed 4% of the sample, non-carbonate values in bed #2 range from 0% to 30%.

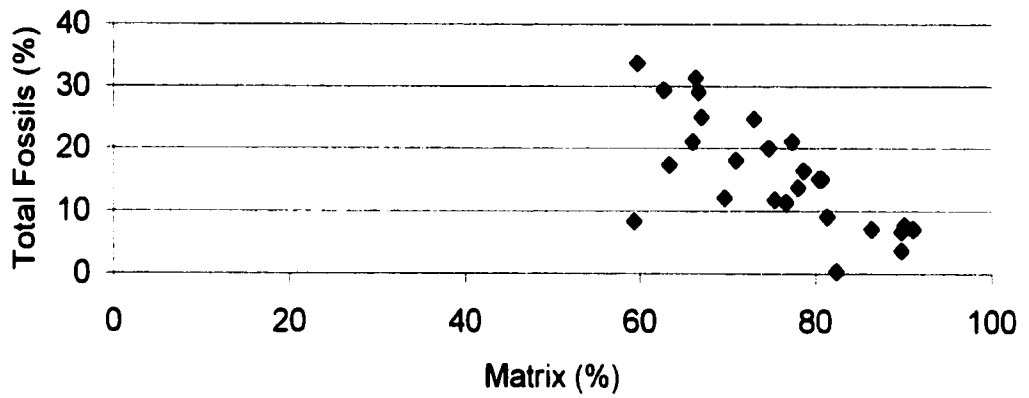
Bed #3, with one exception (sample #37), is very uniform (Fig 15c). Total fossils range from about 10% to 36%, with an average of 24%, and matrix ranges from 61% to 87%, with an average of 72%.

Figure 16 shows the relationship of fossils versus non-carbonate grains in the three limestone beds. These plots show a lot of variability, with fossils ranging from

c) Bed #3



b) Bed #2



a) Bed #1

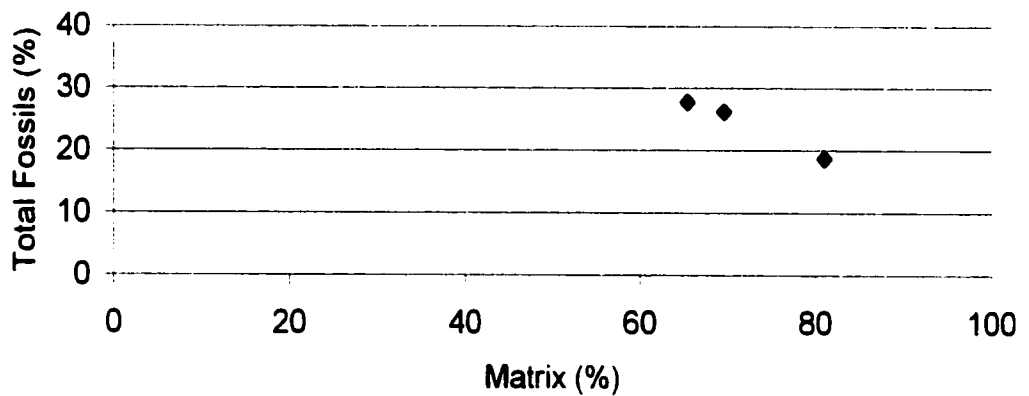
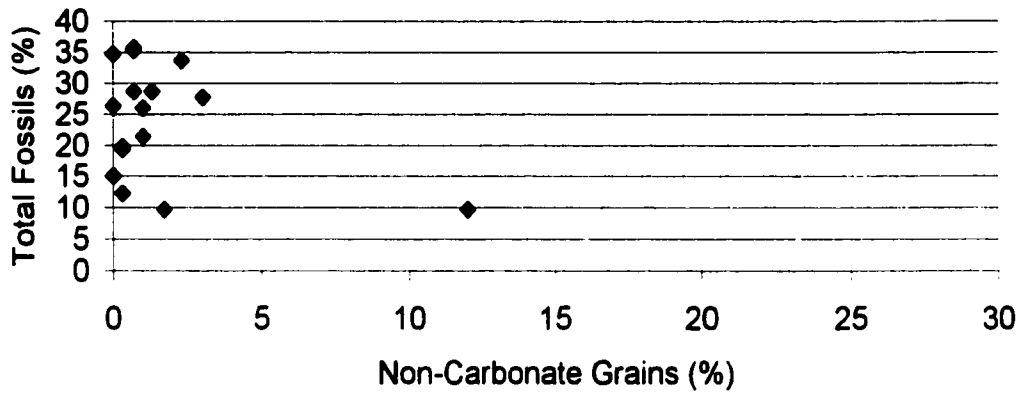
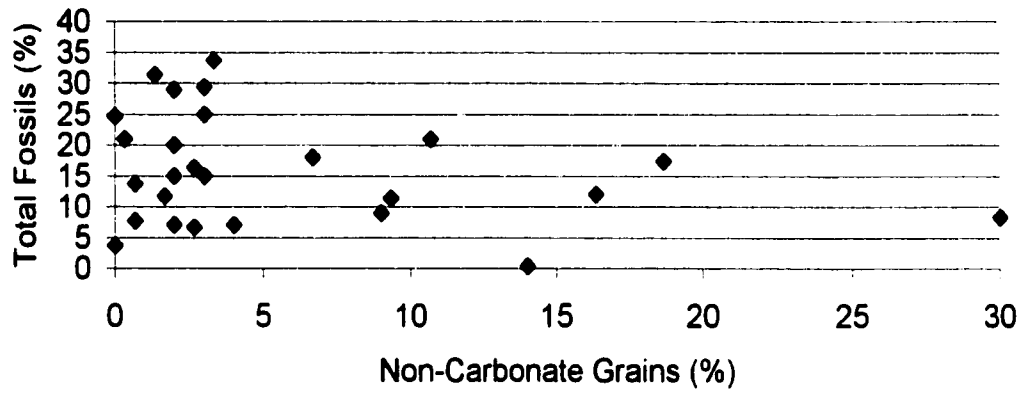


Figure 15. Total fossils versus matrix for limestone beds #1 through #3.

c) Bed #3



b) Bed #2



a) Bed #1

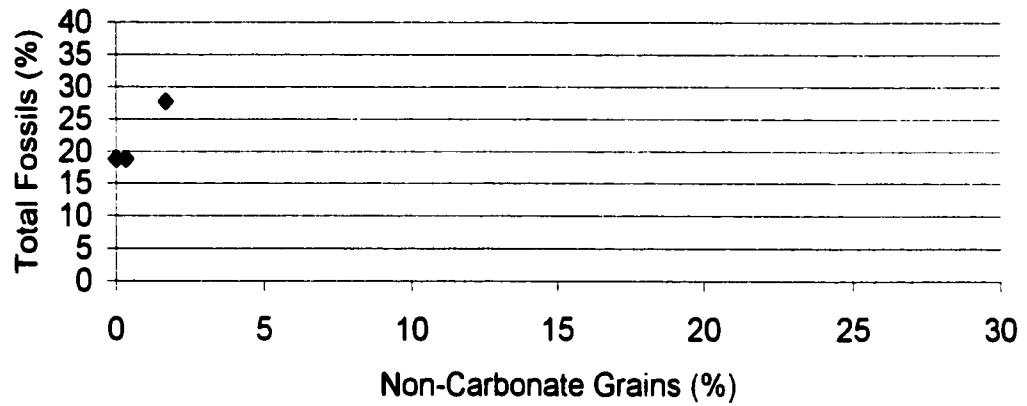


Figure 16. Total fossils versus non-carbonate grains for limestone beds #1 through #3.

0.3% to 36% and non-carbonate percentages ranging from 0 to 30%. There generally is no clear correlation between fossils and non-carbonate grains in these samples.

In the three samples from bed #1, the fossil percentages range from 19% to 28% and non-carbonate percentages range from 0 to 1.7%, with an average of 0.7%. With a 9% increase in fossils, there is only a slight increase in the amount of non-carbonate grains (Figure 16a).

Bed #2 shows the largest variability in the ratio between fossils and non-carbonates in the three beds. Fossils range from 0.3 to 34% and non-carbonate percentages range from 0 to 30%, with an average of 5.7%. Figure 16b shows that there is such large variability in the spread of points that there is no correlation (positive or negative) between the amounts of fossils and the amount of non-carbonate grains present in the bed as a whole.

Of the twenty-six samples from bed #2, five samples have more than 10% sand. Three of these five samples contain predominantly very fine-grained sand and two samples contain predominantly fine-grained sand. Only two samples (#13 and #22) have no counted points of fine-grained sand, very fine-grained sand, or silt.

The fossil contents of most samples from bed #3 are almost as large as those in bed #2, ranging from 10% to 36%. Bed #3 has a small range of non-carbonate grains, predominantly from 0% to 3%, with an average of 1.6%, and one abnormal outlier (sample #37) at about 12% (Fig. 16c). Sample (#37) also has the lowest fossil content (10%), equal only to sample #44 (with 1.7% non-carbonate grains).

Figure 17 shows the relationship of fossils to insoluble residue. Figure 17 is similar to Figure 16, but has a larger component of scatter because the insoluble residue includes silt and clay that were not visible during the petrographic analysis. The fossils range from 0.3% to 36% and insoluble residues range from 0.59% to 41.5%.

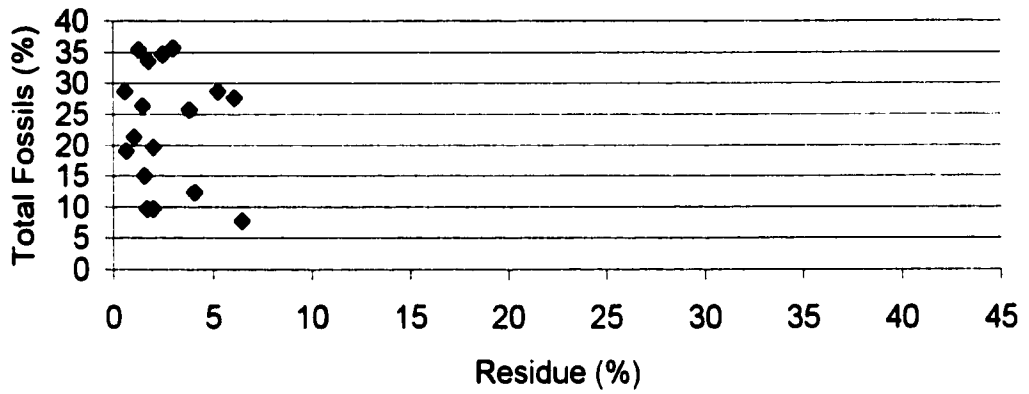
For beds #1 through #3, the fossil percentages are the same as they are in Figure 16. In most cases, the residue values are higher than the values for non-carbonate grains in the same sample. In bed #1, residue ranges from 0.89% to 3.81%. Residue in bed #2 ranges from 2.96% to 41.5%, and that in bed #3 ranges from 0.59% to 6.09%. There is no clear correlation between fossils and insoluble residue in these samples.

Pelecypods and gastropods are the most abundant fossils in these rocks. Figure 18 shows the percentages of pelecypods and gastropods in the three different beds. The fossil percentages were calculated for each sample as a portion of the whole rock (Appendix D).

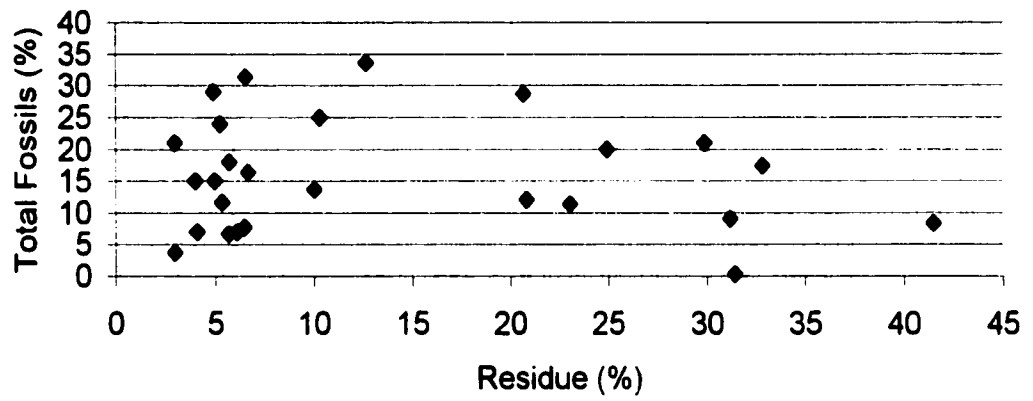
Bed #1 contains predominantly pelecypods (Fig. 18a). A total of 141 pelecypods and 46 gastropods were point-counted in the three samples collected from bed #1, so the ratio of pelecypods to gastropods is about 3:1. In bed #1, pelecypods average about 17% and gastropods average 6.6%.

Although variable throughout bed #2, gastropods make up the majority of the fossils, and most samples have a small percentage of pelecypods (Fig. 18b). From twenty-six samples, a total of 193 pelecypods and 1046 gastropods were point-counted. In bed #2, pelecypods average 2.3% and gastropods average about 14%. In fifteen of the twenty-six samples, pelecypods make up 2% or less of the total sample. Five samples

c) Bed #3



b) Bed #2



a) Bed #1

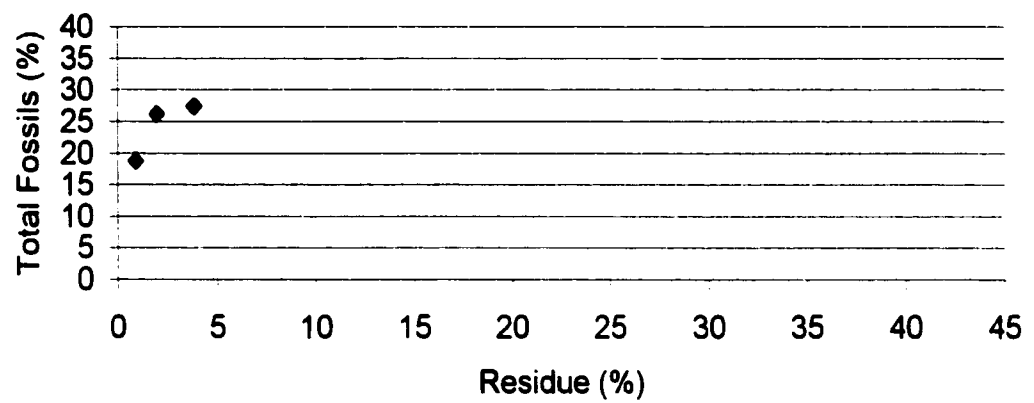
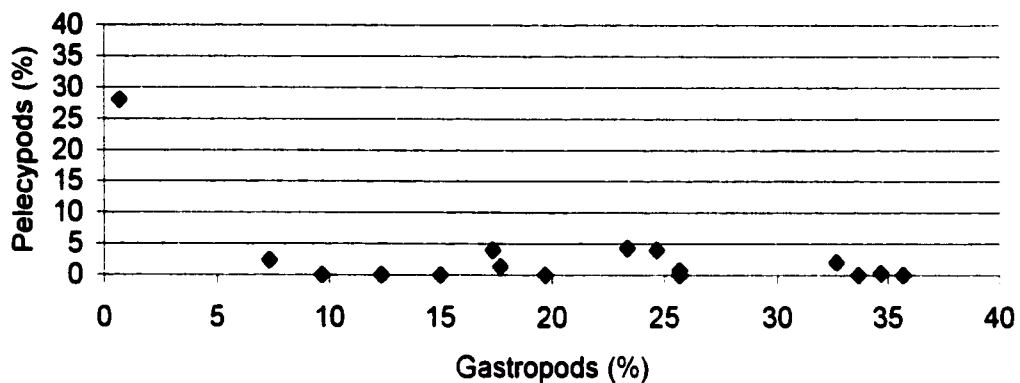
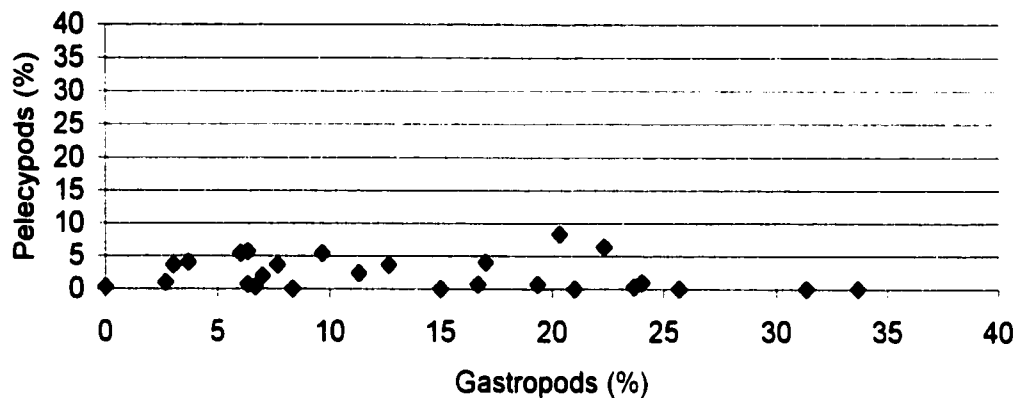


Figure 17. Total fossils versus residue for limestone beds #1 through #3.

c) Bed #3



b) Bed #2



a) Bed #1

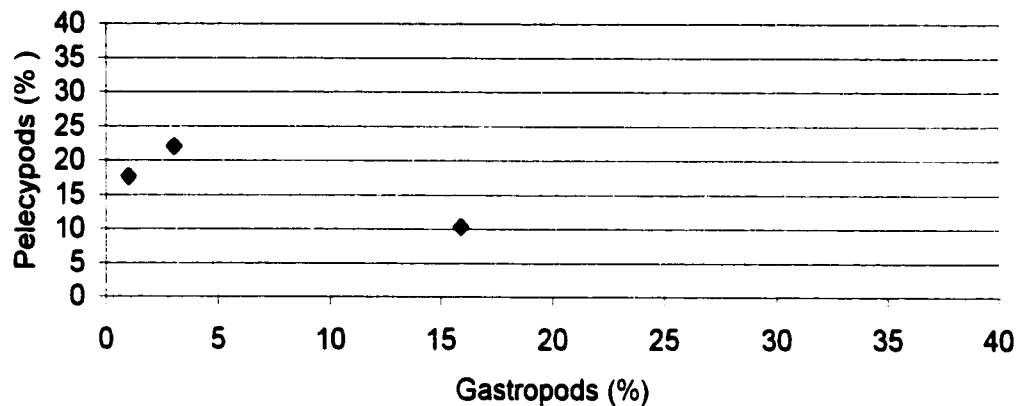


Figure 18: Pelecypods versus gastropods for limestone beds #1 through #3.

have almost equal amounts of pelecypods and gastropods, and three of these samples (#21, #25 and #29) have slightly more pelecypods than gastropods. Twenty-one samples contain predominantly gastropods and five of these samples contain exclusively gastropods.

The fossils in bed #3 are predominantly gastropods (Fig 18c). In bed #3, 141 pelecypods and 1007 gastropods were point-counted in sixteen samples. In bed #3, pelecypods average 1.8% and gastropods average 21%. One sample (#30) contains predominantly pelecypods, but pelecypod percentages in the other samples do not exceed 5% of the total sample, with most of them ranging in value from 0% to 2%.

Figure 19 shows the variation of fossils with distance from east to west along the strike of the beds. There are differences in fossil abundance between beds, but no discernible spatial pattern along strike of the beds. Some samples within meters of each other have differences as much as 15% in the amount of fossils present.

Fossils in bed #1 make up from 19% to 28% of the solid point counts over the length of outcrop (Fig. 19a). The highest and lowest fossil concentrations for this bed are in consecutive samples #1 and #2, respectively.

Bed #2 has the broadest range of fossils (Fig. 19b), with fossil percentages ranging from 0.3% to 34%. Bed #2 also consistently has the largest variation of fossil percentages along the length of the bed. Seventeen of the twenty-six samples have fossil percentages less than 20%.

Bed #3 also has a broad range of fossils (9.7%-36%) (Fig. 19c). Six of the sixteen samples from bed #3 have fossil percentages less than 20% and two of these six samples

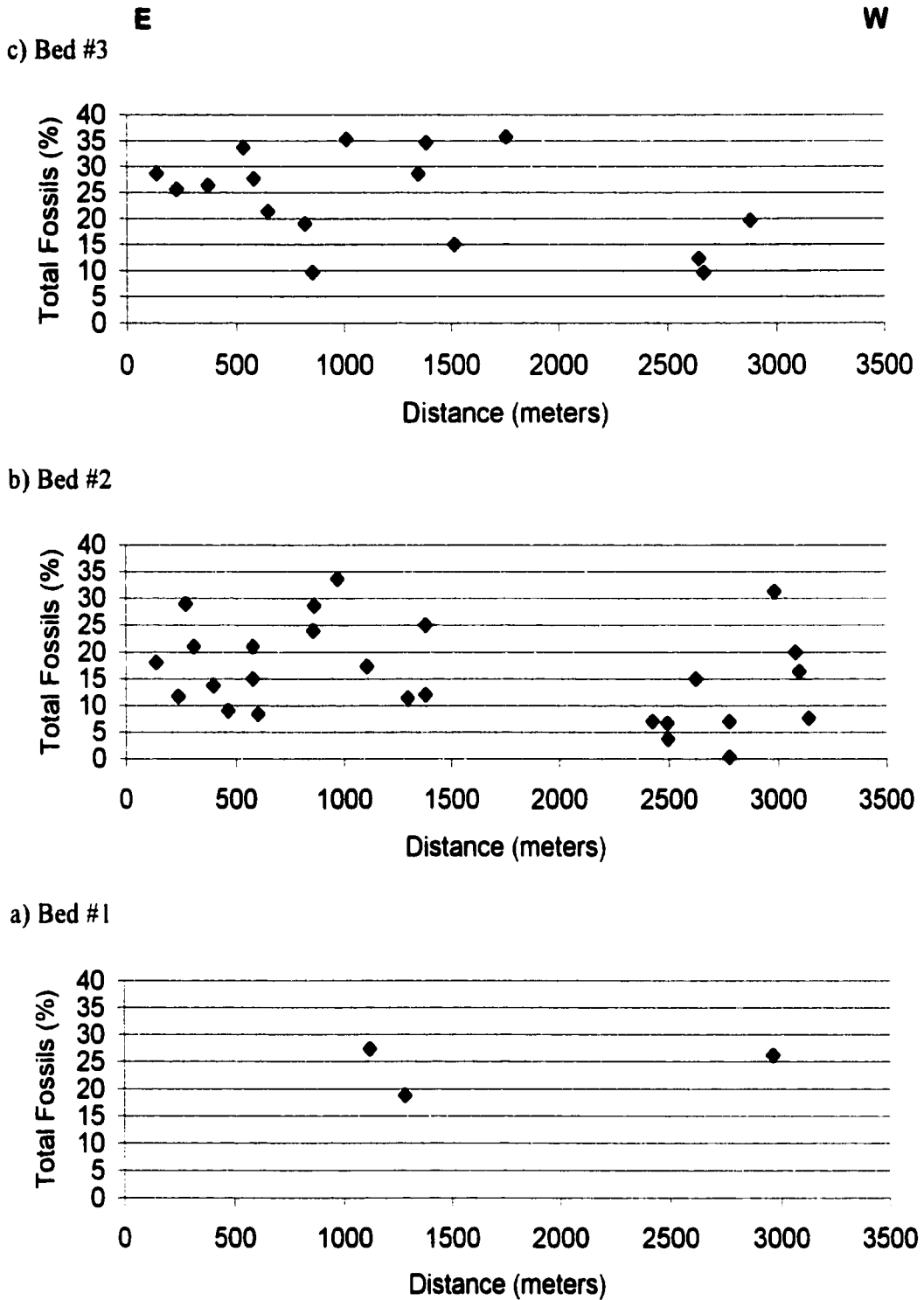


Figure 19. Total fossils versus distance from eastern edge of field area for limestone beds #1 through #3.

have values close to 10%. Bed #3 has higher overall fossil percentages and lower insoluble residues of terrigenous sand and silt (Figs. 10c, 16c) than bed #2.

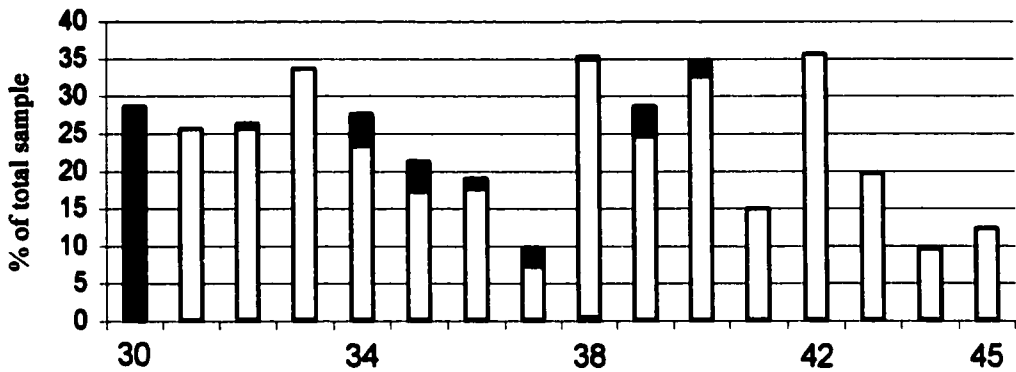
Figure 20 shows the spatial distribution of ostracods, gastropods and pelecypods from samples in the three limestone beds. The proportions of all three fossils are represented as relative percent of the whole solid sample, excluding pore counts. Ostracods range from 0% to 2.3%, gastropods range from 0% to 36% and pelecypods range from 0% to 28%.

Figure 20 shows that pelecypods outnumber gastropods in two out of three samples from bed #1 and in the bed as a whole (Fig. 20a). Ostracods are minor components, only occurring in sample #1, and averaging 2.33% for bed #1. With only three samples, it is difficult to determine any possible spatial patterns in the ostracods, gastropods or pelecypods, or the fossil totals as a whole for bed #1.

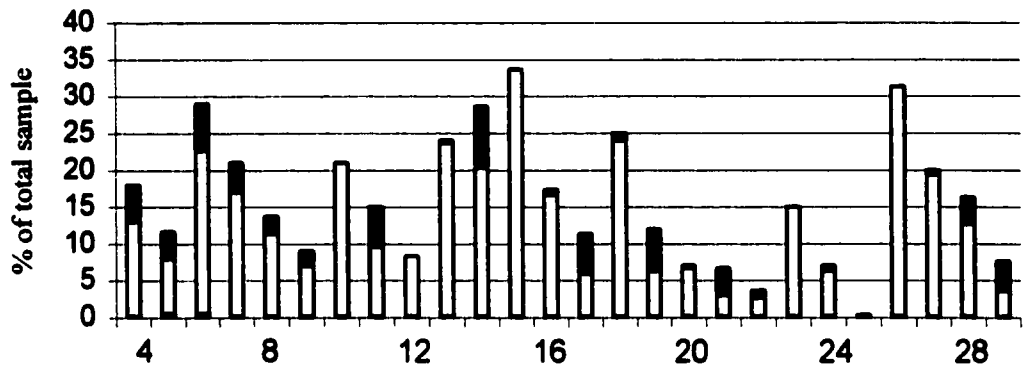
Bed #2 is quite variable in the total amount of fossils present and the relative amounts of the three fossil types present (Figure 20b). Samples #5 and #6 each contain one ostracod, the only ones observed in all of bed #2, averaging 0.03% for bed #2. There are two possible patterns recognizable in bed #2. One pattern is the grouping of samples near the center of the field area (#13 through #18) that have high fossil content (Figure 20b). Sample #17 only has a moderate fossil content of 11%, but the other five samples range from 17% to 34% total fossils. The other pattern is the grouping of samples with very low fossil content (samples #20 through #25), just west of the high grouping. Sample #23 has a moderate fossil content of 15%, but the other five samples range from 0.3% to 7%.

E

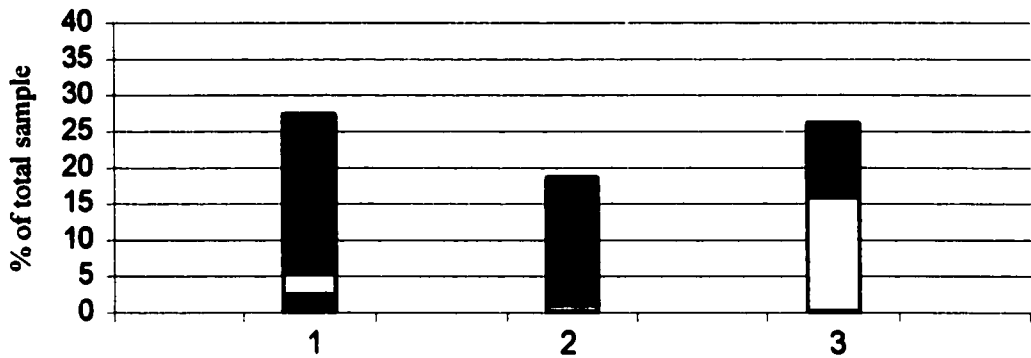
c) Bed #3



b) Bed #2



a) Bed #1



EXPLANATION ■:Ostracods □:Gastropods ■:Pelecypods
 X-axis: Sample #, labeled from east to west, starting from bed #1.

Figure 20: Ostracods, gastropods and pelecypods graphed as percent of total sample. Numbers on horizontal axis refer to specific samples.

In bed #3, ostracods are only present in sample #38, averaging 0.02% for this bed (Fig. 20c). Bed #3 also shows no recognizable pattern in the amount of fossils over the length of the bed.

As can be seen from Figure 20, ostracods are uncommon and very few samples actually contain any ostracods. Bed #1 has the only sample (#1) where seven ostracods were point-counted, representing 2.3% of the total sample. Two samples (#5 and #6) from bed #2 and one sample (#38) from bed #3 each contain one point-counted ostracod, making up less than 1% of the total sample.

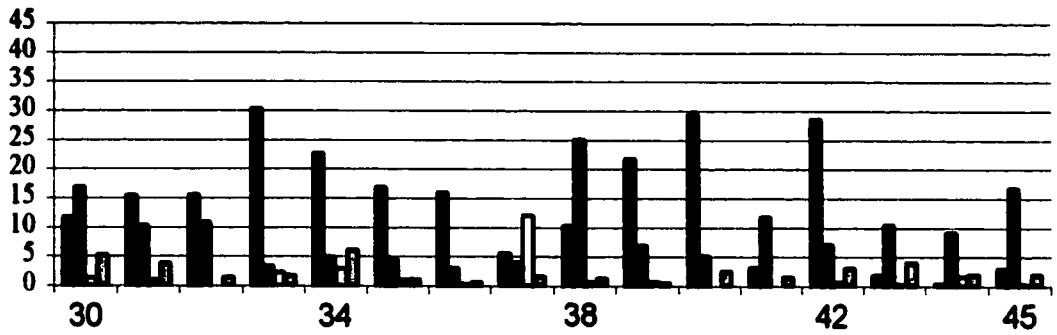
Invertebrate bone pieces also occur within the three limestone beds. Of these, some of the fish bones have been identified as *Stickleback* (Jerry Smith, 1999, oral commun.).

The condition of the fossil shells is variable between the samples and the beds. Figure 21 illustrates the condition of the fossils (intact versus fragmented) and how the amount of fragmentation relates to the amount of non-carbonate grains and insoluble residue present in each sample. In all forty-five samples, only gastropods are observed intact a majority of the time. Only a maximum of ten percent of the pelecypods are intact in any of the samples, and most samples contain fewer than 5% intact pelecypods.

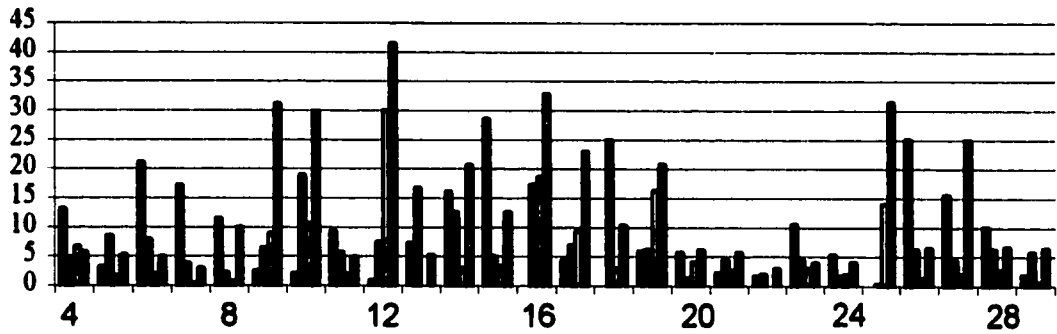
Bed #1 contains fossils that are 92% fragmented (Fig. 21a). The majority of terrigenous material present is predominantly clay (Fig. 21a).

Bed #2 has a mixed assemblage of intact (48%) and fragmented (52%) fossils (Fig. 21b). Half of the samples contain mostly intact fossils and the other half contain mostly fragmented fossils. Of the samples that contain 9% or more non-carbonate sand,

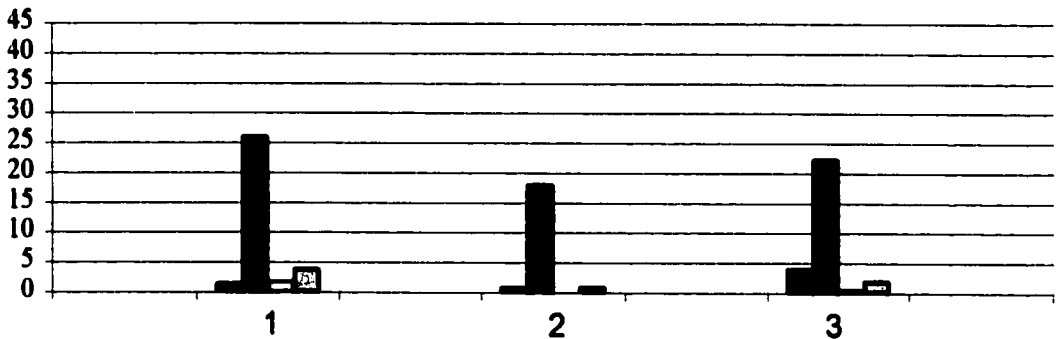
E
c) Bed #3



b) Bed #2



a) Bed #1



EXPLANATION

■ : Intact fossils

□ : Non-carbonate grains

X-axis: Sample number; Y-axis: % of total sample

■ : Fragmented fossils

▣ : Insoluble residue

Figure 21. Abundances of intact and fragmented fossils and non-carbonate components for limestone beds #1 through #3. Numbers on horizontal axis refer to specific samples.

the fossil assemblages are predominantly fragmented. Twenty samples in bed #2 have residue values that are more than twice the non-carbonate values as determined petrographically. It can be concluded, therefore, that clay is the predominant terrigenous material present in these samples. Sample #4 is the exception, with sand (point-count value) exceeding the residue value as the predominant terrigenous material present.

Bed #3 contains 55% intact fossils and 45% fragmented fossils (Fig 21c). Ten of the sixteen samples from bed #3 consist of predominantly intact fossils. Sample #38 is an exception, containing predominantly fragmented gastropods. Samples #30, #31 and #32 contain about equal proportions of intact and fragmented fossils. Clay is the predominant terrigenous material present in ten of sixteen samples (although not the same ten samples as the ones with intact fossils), and sand is the predominant material in the remaining six samples.

Comparison of Data Sets

It is important to determine how well sample values agree between the data for X-ray, insoluble residue and petrography. There are various degrees of accuracy for different analytical methods, and some methods are more definitive for certain parameters than they are for others (Table 1).

X-ray data can be affected by sample preparation and by interference effects caused by the interaction of different minerals. Petrographic analysis can be hampered by the presence of grains that are too fine to see. Insoluble residue, X-ray and petrographic analyses can all be affected by sampling. Beds can be variable vertically

and laterally, producing differences between the data sets. Although X-ray and residue samples were homogenized, the sample used for thin-section is necessarily distinct from samples for other analyses.

The insoluble residue data are individually compared to the X-ray and petrographic data because these data proved to be a good resource for crosschecking against the X-ray data (Table 1). It can be seen from Table 1 that the values for the X-ray data closely match the values for the insoluble residue data, except for two samples. Samples #8 and #27 are from bed #2, and X-ray analyses of these samples indicated only trace amounts of non-carbonates, whereas insoluble residue analysis indicated medium and high amounts, respectively. This indicates that the residue in these samples consists of clay minerals or that there is significant variation between the sub-samples that were analyzed by the two techniques.

By comparing the insoluble residue data with the petrographic (point-count) data for all the samples, both positive and negative discrepancies were observed between these two sets of data (Table 1). Ninety-one percent of the insoluble residue values are higher than the non-carbonate point-count values for the same sample.

Visual inspection of residues from the insoluble residue analysis showed that samples in bed #1 contain clay as the main component of non-carbonate residue. Of the six non-carbonate materials point-counted in all three samples from this bed, only one is a feldspar, two are bone fragments and three were counted as miscellaneous other.

Visual inspection determined that the insoluble residue from thirteen of the twenty-six samples in bed #2 is predominantly silt and clay. Twenty-five of these

samples contain very fine sand to fine sand and eleven contain 10% or more sand.

Residue values in bed #2 are much higher than the petrographically visible non-carbonate grains for samples #8, #9 and #27 (#8 and #27 discussed above), and also for samples #13, #14 and #29 (Table 1). These large discrepancies between high residue values and low point-count values indicate that these samples have non-carbonate residues predominantly composed of clay and/or very fine silt that are not observable using petrographic techniques.

Visual inspection of the residues in bed #3 shows that four of the sixteen samples contain silt and clay. Eight of the sixteen samples contain small amounts of very fine- and fine-grained sand and one has a medium amount of sand.

Residue data with slightly lower values than the non-carbonate point-count data are observed in samples #4, #33, #37 and #39. Sample #37's residue value is much smaller than the point count value (Table 1). X-ray analysis of sample #37 shows a trace amount of quartz, whereas point-count analysis showed 7% quartz. This indicates that sample #37 must be variable and that the thin section was from a sandier part of the bed than the samples prepared for the X-ray and insoluble residue analysis.

Although the X-ray data are not quantitative, relative amounts of the minerals investigated for this study were used to compare with the petrographic data. The X-ray method was able to detect the non-carbonate minerals in small amounts, even when they were not visible during the point-count analysis. The values from X-ray analysis agree with the values determined from point-count analysis with the exception of five samples. Differences between the two sets of data typically occurred where high amounts of quartz

were indicated by X-ray analysis, but very fine-grained quartz was not observed during the point-count analysis. For example, X-ray analysis indicated abundant quartz in samples #9 and #10 from bed #2, whereas point-count values for quartz are moderate, ranging from 6.7% to 8% (Table 1). Common amounts of quartz are indicated by X-ray analysis in samples #14, #15 and #18 from bed #2, but point-count values are low, ranging from 1.0% to 2.7%.

Overall, the insoluble residue is the most reliable technique for determining the amount of siliciclastics in the samples. Point-count analysis is the second most reliable technique, although this technique misses any silt and clay particles present. X-ray is the least reliable technique available for determining the amounts and types of siliciclastics present due to the interference effects produced by the presence of other minerals.

FOSSILS

Dr. Calvin Stevens identified invertebrate fossils in the three limestone beds to genus or in some cases species. This was accomplished by using Hanley's (1976) illustrations of molluscan assemblages from stratigraphic sections in the Wasatch and Green River formations south of the Rock Springs uplift. Fossils identified in the three beds are listed in Table 2. Question marks on fossil identification indicate uncertainty in identification at the species level due to the fragmented nature of those specimens.

Fossils identified in samples from bed #1 include *Biomphalaria aequalis*(?) and *Omalodiscus cirrus*. Although pelecypods are the most abundant fossil present in bed #1, their identification in the samples was difficult; however fossil associations indicate that they are probably *Sphaerium*. Fossils from bed #2 include *Biomphalaria aequalis*(?), *Hydrobia* aff. *H. utahensis*(?), *Omalodiscus cirrus*, *Oreoconus* sp., *Physa bridgerensis*(?), *P. longiuscula*(?), *P. pleromatis*(?) and the previously mentioned vertebrate fossil, *Stickleback* sp. The fossils identified from bed #3 include *Biomphalaria aequalis*, *Biomphalaria storchi*, and *Sphaerium* sp.

Hanley (1976) identified five associations. These associations are *Plesielliptio* (Pl); *Goniobasis-Viviparus* (G-Vi); *Pisidiidae-Goniobasis-Valvata* (Pi-G-V); *Physa-Biomphalaria-Omalodiscus* (P-B-O); and *Oreoconus* (Or) (Hanley, 1976). Fossils in each of the three limestone beds include representatives of the *Physa-Biomphalaria-Omalodiscus* (P-B-O) association and bed #2 also contains the most common terrestrial gastropod of the *Oreoconus* (Or) association.

TABLE 2: TABLE OF IDENTIFIED FOSSILS IN EACH BED

FOSSILS	BED #1	BED #2	BED #3
<u>Gastropods</u>			
<i>Biomphalaria aequalis</i>	?	?	X
<i>Biomphalaria storchi</i>			X
<i>Hydrobia</i> aff. <i>H. utahensis</i>		?	
<i>Omalodiscus cirrus</i>	X	X	
<i>Oreocomus</i> sp.		X	
<i>Physa bridgerensis</i>		?	
<i>Physa longiuscula</i>		?	
<i>Physa pleromatis</i>		?	
<u>Pelecypods (Bivalves)</u>			
<i>Sphaerium</i> sp.	?		X
<u>Ostracods</u>			
	X	X	X
<u>Fish</u>			
<i>Stickleback</i> sp.		X	
<u>EXPLANATION:</u>			
?: Fossil is present, but identification is not confirmed at species level, genus level identification is more probable.			
X: Fossil is present; identification is confirmed at species level, except for <i>Oreocomus</i> , <i>Sphaerium</i> , Ostracod and <i>Stickleback</i> .			

DISCUSSION

The three limestone beds studied were deposited in either oxbow lakes or floodplain ponds as indicated by the presence of a variety of fresh-water fossils of the *Physa-Biomphalaria-Omalodiscus (P-B-O)* assemblage (Hanley, 1976). A more precise interpretation of the environment in which these three limestone beds were deposited is based on the type, size, intactness and distribution of the fossils, the minor components, such as non-carbonate grains and dolomite, and the lateral continuity of beds.

Factors such as the type, size and abundance of fossils, the distribution of non-carbonate grains, and bed color (in one case) also can be used to distinguish the limestone beds. Analysis of the limestone beds in the field and/or in the laboratory can be used to correlate these beds across covered areas.

Depositional Environment

The three limestone beds of this study lie within the main body of the Wasatch Formation, which comprises rocks that were deposited mostly by streams in an intermontane basin upon a broad floodplain (Roehler, 1979). The deposits are characterized by brown and gray fluvial channel sandstones, floodplain alluvial sandstones and mudstones, and lacustrine siltstones, claystones, carbonaceous siltstones and claystones, and some limestones (Savage, 1972).

There are four possible sources of the carbonate in the limestone beds: 1) inorganically precipitated carbonate, 2) photosynthesis-induced, inorganically

precipitated carbonate (or bio-induced carbonate), 3) biogenic carbonate consisting of debris from calcareous plants and animals, and 4) allochthonous (detrital) material derived from carbonate rocks in the drainage basin (Dean and Fouch, 1983). According to Dean and Fouch (1983), most of the carbonate is inorganic or bio-induced in lake sediments, although ostracod- and mollusc-rich layers can also occur. Molluscs and ostracods rarely make up a large component of these three limestones, so the origin of most of the limestone is likely to have been bio-induced by microbial activity.

Interbedded with these three limestone beds are sandstone, siltstone, claystone and shale of varying characteristics and thickness (Fig. 9 and Appendix A). Four of the sandstones contain cross-laminations and other tractive current features, although the majority of the sandstones are massive. The paucity of cross-laminations in most of the beds may be due to bioturbation.

The shale and claystone deposits likely represent distal overbank deposits and/or crevasse splays. The siltstone deposits indicate areas of overbank flows that are closer to the streams than those represented by the shale and claystone deposits. The sandstones, especially the ones with cross-laminations, represent areas of proximal overbank flows and stream levees.

The maximum thickness of the siliciclastic and carbonate deposits studied here (from break in slope at base to ridge top) is 18.25 m at measured section #3 (Fig. 7 and Appendix A). Johnson (1990) determined that the Fort Union – Wasatch – Luman stratigraphic interval along the Rock Springs uplift represents approximately 9 million years of deposition. The thickness of these three formations is about 813.2 m in the field

area (Roehler, 1977). These data indicate an average sedimentation rate of about 9 cm per thousand years. If sedimentation rates were constant over this 9-million-year interval, the sediments in the field area would represent about 200,000 years of deposition.

General Overview

The types and sizes of fossils can be used very effectively to interpret depositional environments as shown by Hanley (1976), who determined different environments of the molluscs from the Wasatch Formation of southwestern Wyoming. Hanley (1976) also determined the biostratonomy of the molluscan assemblages and used the descriptors "in place," "disturbed neighborhood," or "mixed (in-place, or disturbed neighborhood)." These terms reflect the degree of transport of the assemblage. Disturbed-neighborhood assemblages dominate in the Wasatch Formation, and mixed-disturbed-neighborhood and in-place assemblages are second and third in abundance, respectively.

The fossils identified in the three limestone beds belong to the *P-B-O* association, which is indicative of shallow ponded waters and locally impounded water in stream (oxbow lake) habitats (Hanley, 1976). This association includes aquatic pulmonate gastropods, pisidiid bivalves, and gill-breathing gastropods. Recent habitats of coexisting aquatic pulmonates and pisidiid bivalves include shallow ponded waters, locally impounded water in streams, and shallow, even temporary, lentic (quiet water) habitats such as ponds (Hanley, 1976). The large diversity of aquatic pulmonate species (16) in the *P-B-O* association in the Wasatch and Green River formations indicates that the

ponds may not have been ephemeral (Hanley, 1976). Hanley (1976) also noted that the possibility of an oxbow lake habitat could not be excluded on faunal grounds.

The rather large geographic extent of these thin limestone beds (Fig. 8), however, argues against an oxbow lake interpretation. Bed #1 is a minimum of 2.5 km in length and beds #2 and #3 extend at least 3.25 km. In addition, oxbow lakes have point-bar sequences associated with them, and none were observed in the immediate field area (Fig. 9 and Appendix A). Therefore, these beds are interpreted to represent a floodplain pond environment.

The rarity of red beds and the reduction of any iron compounds to gray and green pigments in this floodplain suggest that the soils were moist or saturated (Roehler, 1979). The streams in this area evidently had well-developed levees (Roehler, 1979), and they were probably higher than the surrounding floodplain areas where ponds developed. Overbank floods and crevasse splays also probably contributed water and sediments to the ponds.

The condition of the fossils (intact or fragmented) and the amount of siliciclastics (Fig. 21) were used to ascertain whether a sample belonged to an "in-place," "disturbed-neighborhood" or "mixed" (in-place or disturbed-neighborhood) assemblage (Hanley, 1976). A bias may exist because intact gastropods and fragmented pelecypods are present in the same sample a majority of the time. The intact gastropod shells may indicate deposition *in situ* or they may reflect the durability of the gastropod shells as compared with pelecypod shells and survival during transport.

The plots of fossils versus distance (Fig. 19), relative fossil percent along strike (Fig. 20) and shell intactness versus terrigenous materials along strike (Fig. 21) show no obvious patterns from east to west. Figure 20b shows that bed #2 contains two six-sample groupings that may represent a fossil cluster; each group contains five samples that characterize that group as having either high or low fossil content. Residues (Fig. 10) also show no observable pattern from east to west. This would suggest that proximity to the shore or a delta did not control distribution of fossils or the amount of insoluble residue. Another possibility is that all existing sample locations may be some distance from the original edge of the pond. Large ponds can be very irregular in shape due to existing topography, and present outcrop exposures where samples were collected may have no relationship to the original shoreline.

Plots of fossils against non-carbonate grains (Fig. 16) and fossils against residue (Fig. 17) do not show any observable patterns between abundances of the fossils and the terrigenous materials. Therefore, variations in fossil content and terrigenous materials do not seem to reflect winnowing by currents.

A sheltered embayment containing aquatic plants may have caused the concentration and variation observed in the fossil and siliciclastic contents. Fossil contents could have been influenced by variations in the types and amounts of aquatic plants present. With the presence of an adequate food supply and protection from predators, fossils could become more diverse and/or abundant. In other places, some of the aquatic plants may also have concentrated the siliciclastics by acting as baffles, trapping the incoming sediments or reducing the current enough to cause settling.

One of the more difficult aspects to explain from this field study is the presence of dolomite in some of the samples. Dolomite is present in eleven of the forty-five samples, although nine samples have only trace amounts (Appendix B).

The presence of dolomite in the main body of the Wasatch may be explained by mechanisms similar to those that produced the dolomite that is common within the Green River Formation (Desborough, 1978; Smoot, 1978). Recent models of dolomite formation incorporate anaerobic microbes, including sulfate-reducing bacteria (Burns and others, 2000). Erosion of dolomite crusts from adjacent mudflats (e.g., Wiggins and Harris, 1994) may also be a possible explanation for the dolomite in limestone beds #2 and #3.

Bed #1

The fossils in bed #1 are predominantly pelecypods that could not be identified in the hand-samples due to their fragmented condition. The presence of other elements of Hanley's *P-B-O* association, such as *Biomphalaria aequalis*(?) and *Omalodiscus cirrus*, suggest that these pelecypods are probably *Sphaerium*. The limited fossil assemblage in bed #1 may indicate that this pond experienced fluctuations in the size, chemistry or temperature of the water during deposition.

Bed #1 contains predominantly fragmented fossils (Fig. 21a) and would seem to represent the disturbed-neighborhood assemblage of Hanley (1976). This suggests a moderate-energy environment, but the small amounts of non-carbonate grains and insoluble residues that are predominantly silt and clay (Table 1 and Fig. 21a) may

indicate a low-energy environment. The fragmented condition of the fossils may be due to predation instead of currents.

The low amounts of residue in bed #1 may indicate that sediment influx from stream overbank flow was very low during deposition. A high fossil content (specifically gastropods) may indicate areas where fossils and aquatic plants lived in a sheltered environment.

Bed #2

Physa appears to be the most abundant fossil in bed #2, but *Biomphalaria* is also abundant in some samples. *Omalodiscus*, *Hydrobia* (?) and *Oreoconus* are also present. These fossils in bed #2 represent the classic *P-B-O* association of Hanley (1976), except for *Oreoconus*, which is a terrestrial gastropod. This terrestrial gastropod generally lives in moist, calcium- and organic-rich environments (Hanley, 1976), and the presence of *Oreoconus* in the terrigenous-sediment-rich samples of bed #2 suggests that these terrestrial gastropods were probably washed into the pond along with the sediment. *Physa pleromatis*, which may be present in bed #2, is also a rare component of Hanley's *Plesielliptio* association and is characteristic of flowing water habitats. Introduction of this fossil into bed #2 may have been due to stream input.

Of the vertebrate bones present in bed #2, *Stickleback* was identified. Modern descendants of this fish typically inhabit quiet water and live among a wide variety of heavy aquatic plants, where they feed on small invertebrates. They generally do not live in turbid water, because they are visual feeders (Moyle, 1976). The diverse fossil

assemblage and the presence of *Stickleback* in bed #2 indicate a quiet, very stable pond environment.

Bed #2 contains a mixture of intact and fragmented fossils (Fig. 21b). The samples with predominantly intact fossils may represent the in-place assemblage of Hanley (1976), whereas the samples of predominantly fragmented fossils may represent the disturbed-neighborhood assemblage. The samples with approximately equal amounts of intact and fragmented fossils may represent the mixed assemblage.

Four samples from bed #2 with more than 15% fossils also have insoluble residues over 20% (Fig. 21b) and much of the residue is fine-grained silt and clay. Normally a high terrigenous influx is not conducive to life. Explanations for this association may involve either the shells being moved (slightly) after death into areas of high siliciclastics or deposition of the terrigenous sediment after the animals' death.

There are a couple of possible explanations for the areas of high residue content in bed #2. One explanation is that these may have been areas of stream input (delta) or overbank deposition. Many consecutive samples have very high residue values followed geographically by very low residue values (Fig. 21). These variable high and low residue values may represent a slice through the distal toe of a delta or they may represent areas of overbank deposition that may or may not have been later reworked by currents. Seven samples in bed #2 have fine-grained terrigenous materials that are concentrated in the same areas (samples) as the fossils (Figs. 16, 17), which would suggest that the concentrations of sand and fossils were not from simple winnowing by currents into areas of higher and/or lower wave energy. Concentrations of fossils in samples with little

terrigenous material may represent areas within the pond that were sheltered and contained abundant aquatic plants. High amounts of fossils together with terrigenous sediments may indicate areas where overbank deposits or delta lobes were deposited. The high influx of terrigenous sediments may have killed off the local fauna or post-mortem shells may have been transported to this site contemporaneous with the deposition of the sediments.

Eight of the samples with trace amounts of dolomite are from bed #2 (Appendix B, Table 1). These eight samples are randomly scattered along the length of the bed. Dolomite is present in the Wasatch Formation above and below the three limestone beds in the field area (Dave Andersen, 2000, oral commun.). The dolomite could be detrital, derived from crusts in adjacent mudflats (Smoot, 1978; Wiggins and Harris, 1994) or from older floodplain pond deposits that had been dolomitized.

Bed #3

The fossils from bed #3 are predominantly the gastropods *B. aequalis* and *B. storchi*. *Sphaerium* sp. is another fossil identified in bed #3. Sample #30 is unusual because it contains predominantly pelecypods (Fig. 20c). Conditions may have been more favorable for pelecypod development or the pelecypod shells may have been transported to this site. The fossil assemblage from bed #3 is intermediate between those of beds #1 and #2. This may indicate that this pond experienced minor fluctuations in the size, chemistry or temperature of the water during deposition.

Seven samples from bed #3 contain predominantly intact fossils, four contain about equal proportions of intact and fragmented fossils, and five samples contain predominantly fragmented fossils (Fig. 21c). This suggests that this bed represents in-place, mixed and disturbed-neighborhood assemblages, respectively (Hanley, 1976). Three of the samples with predominantly fragmented fossils (samples #43, #44 and #45) are concentrated at the western end of the field area (Fig. 21c) and may indicate higher energy conditions or more predation at this end of the pond.

The low amounts of residue in bed #3 may indicate that sediment influx from stream or overbank deposits was very low during the deposition of this bed. This may have been due to local variations within the floodplain or to a relatively large distance to the edge of the pond. As in bed #2, high fossil content is not correlated with a high content of non-carbonate grains. As in bed #1, a high fossil (gastropod) content may indicate areas where aquatic plants were prolific in a sheltered environment.

In the three samples with dolomite from bed #3, sample #45 has trace amounts, whereas samples #43 and #44 have abundant amounts (Table 1). It is difficult to interpret the origin of the dolomite in these three samples from this pattern. These are also the same three samples that contain an unusually high content of fragmented fossils compared to the remainder of the bed (Fig. 21c). These fossils may have been fragmented during diagenesis or by normal mechanical processes. The dolomite in samples #43 and #44 was either formed *in-situ* or was detrital, derived from dolomite mudflat crusts or from local Eocene dolomite beds. Dolomite is common in the overlying Green River Formation, and the chemistry of the waters in the Washakie basin

may have been adequate to precipitate dolomite when in the presence of the right combination of elements. Similar conditions may have been present in the Wasatch Formation.

Summary

The three limestone beds studied here are interpreted to have been deposited in floodplain ponds because beds are laterally extensive and contain diverse and distinctive fossil assemblages that are associated with pond environments. The micrite in the three limestone beds was probably bio-induced from microbial activity. The associated siliciclastics are representations of levee deposits and proximal and distal deposits of overbank floods and crevasse splays. Long-term sedimentation rates calculated for these deposits are on the order of 9 cm per thousand years, suggesting that the deposits in the field area represent roughly 200,000 years of accumulation.

The distribution of terrigenous sediment and fossils throughout the limestone beds does not show any kind of pattern that is easy to interpret. Simple winnowing or even the proximity to the shore does not explain the distribution of terrigenous materials and/or fossils. Concentrations of terrigenous materials in bed #2 may be due to overbank floods. Streams may have washed in the terrestrial *Oreocornus*. Other factors such as the geometry of the pond or the presence or absence of aquatic plants in some areas may have influenced the distribution of terrigenous materials and/or fossils. Some sheltered areas could have been favorable for the development of communities of molluscs and aquatic plants, and in other areas the aquatic plants may have acted as baffles, possibly

trapping incoming sediments or reducing the current enough to cause settling of the siliciclastics. The observation that in about half the samples in bed #2 the fossils are predominantly fragmented may indicate either predation or a moderate energy environment, and the association of fossils shows that they were thriving in this shallow pond environment, even in areas of high sediment input. Three samples with unusually high amounts of fragmented fossils in bed #3 are also the only samples in this bed that contain trace to abundant dolomite. The dolomite in bed #3 possibly is detrital or formed *in situ*, and that in bed #2 may be detrital.

Distinctive Features of Beds

The three limestone beds studied here were compared with limestone beds mapped on the Sand Butte Rim NW and Antelope Flats 7-1/2" quadrangles by Roehler (1977) and Roehler and Valcarce (1978), respectively. From the number and location of limestone beds described in the composite stratigraphic sections of Roehler and Valcarce, it is apparent that they did not map all the limestone beds cropping out in the field. Roehler and Valcarce (1978) described a brown silty limestone (fifth limestone above marker bed "B") containing *Physa*, which appears to correlate with bed #2 of this study. Marker bed "A" in the Sand Butte Rim NW quadrangle corresponds to limestone bed #3 of this report, which also corresponds to the "T" limestone of Savage and others (1972).

One of the purposes of this study was to determine whether or not the limestone beds are distinctive enough, either in the field or in the lab, that they could be used to correlate sections across large unexposed stretches. Although the colors and textures of

each bed may change laterally, there are distinctive features that can be used to correlate these beds in the field and in the lab. One useful tool for doing this is by analysis of the non-carbonate grains and insoluble residue.

Bed #2 is the easiest to distinguish because of the wide range and locally high amounts of terrigenous material within this bed (Table 1 and Fig. 10). By comparison, both beds #1 and #3 consistently have low amounts of terrigenous material.

Another feature that can be used to differentiate bed #2 from beds #1 and #3 is its distinctive fossil assemblage. Three fossils in this assemblage, not identified in either of the other two beds, are *Oreocomus*, *Physa* and a high-spined gastropod (Fig. 13), possibly *Hydrobia*. The large size and abundance of *Physa* and the presence of *Oreocomus* are probably the most characteristic features of the fauna of bed #2.

Bed #1 and bed #3 both have small amounts of terrigenous materials, and bed #1 has the smaller average amount of the two (Figs. 10, 16 and 17). The dark to light gray color in the field (Appendix A) and predominance of pelecypods in bed #1 can be used for correlation and differentiation from bed #3.

CONCLUSIONS

Study of the sedimentology, paleontology and petrography of three limestone beds in the main body of the Wasatch Formation in the northwest Washakie basin of Wyoming indicates deposition within floodplain ponds. Each bed contains different fossil assemblages and varying amounts of siliciclastics. Calculated average sedimentation rates suggest that the stratigraphic interval studied represents roughly 200,000 years.

All three of the limestone beds consist primarily of biomicrites with a few samples that are fossiliferous micrites. All of the samples contain calcite, and eleven samples contain dolomite. There are numerous attributes of the three limestone beds that can be used to differentiate between the beds and to correlate each bed throughout the area, including the size, types, and relative abundance of invertebrate fossils, the amount and type of insoluble residues present, and the color.

Bed #1 is dark to light gray in color and is characterized by low amounts of siliciclastics that do not exceed 4% of the sample and fossils that include *Biomphalaria aequalis(?)* and *Omalodiscus cirrus*. A fairly stable pond environment is indicated by the low amount of clastics and limited fossil assemblage.

Bed #2 is variable in color, but is characterized by variable amounts of siliciclastics that range from 3% to more than 41% and fossils that include *Physa(?)* sp., *Biomphalaria aequalis(?)*, *Omalodiscus cirrus*, *Hydrobia* aff. *H. utahensis(?)*, *Oreocomus* sp., and *Stickleback* sp. The diverse invertebrate fossil assemblage and the presence of

Stickleback sp. in bed #2 indicate a quiet, very stable pond environment. Minor amounts of dolomite in bed #2 possibly are detrital in origin.

Bed #3 is also variable in color, but is characterized by low amounts of siliciclastics that do not exceed 6.1% and fossils that include *Biomphalaria aequalis*, *Biomphalaria storchi*, and *Sphaerium* sp. The small amount of clastics and limited fossil assemblage in bed #3 indicates a stable to fairly stable pond environment. The abundant dolomite present towards the western end of the field area may indicate *in situ* formation.

It can be concluded that the depositional environment for these three limestone beds was that of floodplain ponds with abundant aquatic plants and quiet water settings. Conditions during deposition of each bed, however, were different, resulting in different amounts of siliciclastics and different faunas. The differences in the amounts of siliciclastics and in the fossil assemblages should allow recognition and correlation of limestone beds within this part of the Wasatch Formation throughout their extent.

REFERENCES CITED

- Bird, P., 1984, Laramide crustal thickening in the Rocky Mountain foreland and Great Plains: *Tectonics*, v. 3, p. 741-758.
- Bown, T. M., and Kraus, M. J., 1981, Lower Eocene alluvial paleosols (Willwood Formation, northwest Wyoming, U. S. A.) and their significance for paleoecology, paleoclimatology, and basin analysis: *Paleogeography, Paleoclimatology, Paleoecology*, v. 34, p. 1-30.
- Bradley, 1964, Geology of the Green River Formation and associated Eocene rocks in southwestern Wyoming and adjacent parts of Colorado and Utah: U. S. Geological Survey Professional Paper 496-A, p. A1-A86.
- Burns, S. J., McKenzie, J. A., and Vasconcelos, C., 2000, Dolomite formation and biogeochemical cycles in the Phanerozoic: *Sedimentology*, v. 47, Suppl. 1, p. 49-61.
- Coney, P. J., 1978, Mesozoic-Cenozoic Cordilleran plate tectonics, *in* Smith, R. B., and Eaton, G. P., eds., *Cenozoic tectonics and regional geophysics of the western Cordillera*: Geological Society of America Memoir 152, p. 33-50.
- Dean, W. E., and Fouch, T. D., 1983, Lacustrine environment, *in* Scholle, P. A., Bebout, D. G., and Moore, C. H., eds., *Carbonate depositional environments*: American Association of Petroleum Geologists Memoir 33, p. 97-130.
- Desborough, G. A., 1978, A biogenic-chemical stratified lake model for the origin of oil shale of the Green River Formation: An alternative to the playa-lake model: *Geological Society of America Bulletin*, v. 89, p. 961-971.
- Dickinson, W. R., Klute, M. A., Hayes, M. J., Janecke, S. U., Lundin, E. R., McKittrick, M. A., and Olivares, M. D., 1988, Paleogeographic and paleotectonic setting of Laramide sedimentary basins in the central Rocky Mountain region: *Geological Society of America Bulletin*, v. 100, p. 1023-1039.
- Dunham, R. J., 1962, Classification of carbonate rocks according to depositional texture, *in* Hamm, W. E., ed., *Classification of carbonate rocks*: American Association of Petroleum Geologists Memoir 1, pp. 108-121.
- Engebretson, D. C., Cox, A., and Thompson, G. A., 1984, Correlation of plate motions with continental tectonics: Laramide to Basin-Range: *Tectonics*, v. 3, p. 115-119.

- Folk, R. L., 1980, *Petrology of sedimentary rocks*: Hemphill Publishing Company, Austin, Texas, 182 p.
- Goddard, E. N., Trask, P. D., DeFord, R. K., and Rove, O. N., 1963, *Rock-color chart*: The Geological Society of America, New York, 11 p.
- Hanley, J. H., 1976, Paleosynecology of nonmarine Mollusca from the Green River and Wasatch formations (Eocene), southwestern Wyoming and northwestern Colorado, *in* Scott, R. W., and West, R. R., eds., *Structure and classification of paleocommunities*: Dowden, Hutchinson, and Ross, Stroudsburg, p. 235-261.
- Johnson, P. L., 1990, Laramide basin subsidence and fluvial architecture of the Fort Union and Wasatch Formations, southern Green River basin, Wyoming [M.S. thesis]: San Jose State University, San Jose, California, 146 p.
- Keffer, W. R., 1965, *Stratigraphy and geologic history of the uppermost Cretaceous, Paleocene, and lower Eocene rocks in the Wind River basin, Wyoming*: U. S. Geological Survey Professional Paper 495-A, 77 p.
- Kirschbaum, M. A., Andersen, D. W., Baldwin, R. J., and Helm, R. L., 1994, Paleocene drainage systems, Rock Springs uplift, Wyoming: *The Mountain Geologist*, v. 31, p. 19-28.
- Leopold, E. B., and MacGinitie, H. D., 1972, Development and affinities of Tertiary floras in the Rocky Mountains, *in* Graham, A., ed., *Floristics and paleofloristics of Asia and eastern North America*: Elsevier, Amsterdam, p. 147-200.
- Love, J. D., and Christiansen, A. C., compilers, 1985, *Geologic map of Wyoming*: U.S. Geological Survey, scale 1:500,000.
- Lumsden, D. N., 1979, Discrepancy between thin-section and X-ray estimates of dolomite in limestone: *Journal of Sedimentary Petrology*, v. 49, p. 429-436.
- McGrew, P. O., 1971, *The Tertiary history of Wyoming*: Wyoming Geological Association, 23rd Annual Field Conference Guidebook, p. 79-86.
- Mineral Powder Diffraction Data Book*, 1980: International Centre for Diffraction Data, Swarthmore, Pennsylvania, 1396 p.
- Mineral Powder Diffraction Search Manual*, 1974: International Centre for Diffraction Data, Swarthmore, Pennsylvania, 484 p.
- Moyle, P. B., 1976, *Inland fishes of California*: University of California Press, Berkeley, California, 405 p.

- Prichinello, K. A., 1971, Earliest Eocene mammalian fossils from the Laramie basin of southeast Wyoming: Wyoming University Contributions to Geology, v. 10, p. 73-87.
- Roehler, H. W., 1961, The Late Cretaceous-Tertiary boundary in the Rock Springs uplift, Sweetwater County, Wyoming: Wyoming Geological Association, 16th Annual Field Conference Guidebook, p. 96-100.
- Roehler, H. W., 1977, Geologic map of the Sand Butte Rim, NW, quadrangle, Sweetwater County, Wyoming: U.S. Geological Survey Map GQ-1362, scale: 1:24,000.
- Roehler, H. W., 1979, Geological and energy resources of the Sand Butte Rim NW quadrangle, Sweetwater County, Wyoming: Geological Survey Professional Paper 1065-A, 55 p.
- Roehler, H. W. and Valcarce, J., 1978, Geologic map of the Antelope Flats, quadrangle, Sweetwater County, Wyoming: U.S. Geological Survey Map GQ-1437, scale: 1:24,000.
- Savage, D. E., Waters, B. T., and Hutchison, J. H., 1972, Wasatchian succession at Bitter Creek station, northwestern border of the Washakie basin, Wyoming: Society of Vertebrate Paleontology, Field Conference Guidebook, 7 p.
- Sklenar, S. E., 1982, Genesis of an Eocene lake system within the Washakie Basin of southwestern Wyoming [M.S. thesis]: San Jose State University, San Jose, California, 89 p.
- Sklenar, S. E., and Andersen, D. W., 1985, Origin & early evolution of an Eocene lake system within the Washakie Basin of southwestern Wyoming *in* Flores, R. M., and Kaplan, S. S., eds., Cenozoic paleogeography of west-central United States: Rocky Mountain Section S.E.P.M., Denver, Colorado, p. 231-246.
- Smoot, J. P., 1978, Origin of the carbonate sediments in the Wilkins Peak Member of the lacustrine Green River Formation (Eocene), Wyoming, U.S.A. *in* Matter, A. and Tucker, M. E., eds., Modern and ancient lake sediments: International Association of Sedimentologists Special Publication #2, p. 109-127.
- Snoke, A. W., 1997, Geologic history of Wyoming within the tectonic framework of the North American cordillera, *in* Snoke, A. W., ed., Geology of Wyoming: Wyoming State Geological Survey Memoir 5, p. 2-56.

- Sullivan, R., 1980, A stratigraphic evaluation of the Eocene rocks of southwestern Wyoming: Geological Survey of Wyoming, Report of Investigations #20, 50 p.
- Surdam, R. C., and Wolfbauer, C. A., 1975, Green River Formation, Wyoming: A playalake complex: Geological Society of America Bulletin, v. 86, p. 335-345.
- Wiggins, W. D., and Harris, P. M., 1994, Lithofacies, depositional cycles, and stratigraphy of the lower Green River Formation, southwestern Uinta Basin, Utah, *in* Lomado, A. J, Schreiber, B. C., and Harris, P. M., eds., Lacustrine reservoirs and depositional systems: SEPM Core workshop #19, p. 105-141.

APPENDIX A: DESCRIPTION OF MEASURED SECTIONS

The first three of four stratigraphic sections of a portion of the main body of the Wasatch Formation were measured in the Antelope Flats 7-1/2 minute quadrangle, Sweetwater County, Wyoming. The fourth stratigraphic section of a portion of the main body of the Wasatch Formation was measured from the Sand Butte Rim NW 7-1/2 minute quadrangle, Sweetwater County, Wyoming into the Antelope Flats 7-1/2 minute quadrangle, Sweetwater County, Wyoming.

Section 1

Stratigraphic section was measured from the NW 1/4, SE 1/4, SW 1/4 sec. 5, T. 17 N., R. 99 W. to the top of section, located in the SW 1/4, SW 1/4, SW 1/4 sec. 5, T. 17 N., R. 99 W., Antelope Flats 7-1/2 minute quadrangle, Sweetwater County, Wyoming.

Top of section: Unit generally forms ridge tops with overlying rocks separated by a large, covered saddle area.

		Unit Thickness (Meters)	Cumulative Thickness (Meters)
11.	Limestone, bed #3, light-gray, very pale-orange and pale-grayish-orange, massive, crystalline; minor, large, intact gastropods with minor fossil fragments, weathers pale yellow, light grayish orange pink and yellowish brown, irregular lower contact with siltstone and claystone	0.30+	10.55+
10.	Siltstone and claystone, light-gray	3.20	10.25
9.	Sandstone, pale-olive, massive; well-sorted (without micas), moderate to poorly-sorted inclusive of micas, fine to very fine quartz and feldspars, medium to coarse micas, well-cemented	0.15	7.05
8.	Shale, dark-gray, silty, some claystone, some parts are flaky	3.09	6.90
7.	Limestone, bed #2, very pale to pale-grayish-orange, very pale-orange and pale-pinkish-gray, massive; gastropod-rich with minor fossil fragments, weathers pale yellow, yellow and yellowish gray	0.08	3.81
6.	Siltstone and claystone, olive-gray, flaky; siltstone and soft, crumbly, claystone more indurated towards the top, upper contact not distinct	1.48	3.73

	Unit Thickness (Meters)	Cumulative Thickness (Meters)
5. Shale, red, flaky to papery	0.25	2.25
4. Siltstone, pale-yellow, flaky and crumbly; interbedded with 2-cm-thick beds of very fine sandstone, grades upsection into dark gray, flaky siltstone with some very fine sandstone which then grades into yellow siltstone; more interbeds of very fine, silty sandstone, to dark-gray siltstone at the top . . .	0.40	2.00
3. Sandstone, olive-gray, massive, very well sorted; some micas, erosional upper and lower contacts, well-cemented . . .	0.10	1.60
2. Sandstone, light-gray, grading upwards to gray, then yellow at the 1 meter mark for 10-cm, then grades upwards in to a light, friable, gray, sandstone	1.35	1.50
1. Shale, gray, crumbly	0.15	0.15
Total thickness of section 1		10.55+

Base of section: Terminated at the top of a marker red-bed in a lower portion of the main body of the Wasatch Formation. Covered below.

Section 2

Stratigraphic section was measured from the NW 1/4, NW 1/4, NE 1/4 sec. 7, T. 17 N., R. 99 W. to the top of section, located in the NE 1/4, NW 1/4, NE 1/4 sec. 7, T. 17 N., R. 99 W., Antelope Flats 7-1/2 minute quadrangle, Sweetwater County, Wyoming.

Top of section: Unit forms ridge tops with overlying rocks separated by a wide saddle area in a portion of the main body of the Wasatch Formation.

	Unit Thickness (Meters)	Cumulative Thickness (Meters)
24. Limestone, bed #3, pale-yellowish-brown, massive, crystalline; minor 0.5-mm gastropods, weathers light gray to yellowish brown	0.20+	17.71+
23. Shale and siltstone, yellowish-brown to dark-gray, crumbly, weathered	2.60	17.51
22. Sandstone, light-gray to light-red at the top, a 2-cm clay layer at 15.1 m and a 1-cm clay layer at 15.0 m	0.50	14.91
21. Siltstone, sandy, light-gray, flaky habit; minor, very fine sand, siltstone at the top of the bed	1.30	14.41

		Unit Thickness (Meters)	Cumulative Thickness (Meters)
20.	Sandstone, mottled light-red and pale-brown, layer is discontinuous	0.45	13.11
19.	Siltstone and sandstone, pale-brown to yellow, very fine sand, minor cross laminations, rip-up clasts and flame structures . . .	2.25	12.66
18.	Limestone, bed #2, yellowish-gray to light-yellowish-gray and pale-grayish-orange to very pale-grayish-orange, massive, fractured; weathers yellow to yellowish gray and pale yellow .	0.30	10.41
17.	Sandstone, gray, very fine sand, grades upwards into clay-rich siltstone	0.40	10.11
16.	Sandstone, yellow, weathered	0.30	9.71
15.	Siltstone, gray, poorly cemented, grades up into a very fine, very-poorly cemented sand 40-cm to 70-cm thick at the top, erosional upper boundary	1.10	9.41
14.	Sandstone, gray, friable, grades into soft, weakly-cemented sand towards the top, erosional upper boundary	0.20	8.31
13.	Sandstone, light-gray with a 1-cm dusky-red layer at the top .	0.30	8.11
12.	Sandstone, red, with clay rip-up clasts and flame structures, erosional top and bottom contacts	1.00	7.81
11.	Shale, light-gray, flaky	0.88	6.81
10.	Limestone, bed #1, medium-dark to dark-gray and pale-yellow bottom layer, light-gray top layer, fossiliferous, closely-packed fossil fragment layer at the bottom; weathers pale yellow, yellowish light-gray and pale olive; fossils are black in color .	0.03	5.93
9.	Shale, light-gray, crumbly	0.55	5.90
8.	Shale, interbedded, thin, red shale with gray shale and claystone	1.30	5.35
7.	Shale, bands of gray and dark-gray, flaky, crumbly material turning pale-yellow towards the top	0.60	4.05
6.	Sandstone, reddish-brown	0.10	3.45
5.	Shale, loose material, partly covered	1.47	3.35
4.	Sandstone, reddish-brown	0.08	1.88
3.	Siltstone, sandy, and sandstone, silty, yellow	0.92	1.80
2.	Sandstone, gray	0.13	0.88
1.	Shale and siltstone, olive-gray shale, reddish-gray siltstone, alternating layers	0.75	0.75
Total thickness of section 2			17.71+

Base of section: Terminated at the top of red-bed in a lower portion of the main body of the Wasatch Formation, but not the same red-bed as used for the base of section 1.

Section 3

Stratigraphic section was measured from the SE 1/4, SE 1/4, NE 1/4 sec. 12, T. 17 N., R. 100 W. to the top of section, located in the SE 1/4, NE 1/4, SE 1/4 sec. 12, T. 17 N., R. 100 W., Antelope Flats 7-1/2 minute quadrangle, Sweetwater County, Wyoming.

Top of section: Unit forms ridge top in this area with overlying rocks separated by an extensive saddle area in a portion of the main body of the Wasatch Formation.

	Unit Thickness (Meters)	Cumulative Thickness (Meters)
13. Limestone, bed #3, mottled-yellow and light-gray, massive; rare, fossil fragments, carbonaceous, weathers reddish yellow	0.10+	18.25+
12. Covered	9.25	18.15
11. Limestone, bed #2, light-gray to pale-yellow to very pale-grayish-orange, massive, crystalline; minor, mm-size gastropods at top, minor, large, intact gastropods at bottom, partially fractured, weathers pale yellow	0.40	8.90
10. Siltstone and shale, dark-gray towards the top with a 10-cm light-brown siltstone layer at the top of bed	1.25	8.50
9. Sandstone, mottled reddish-brown to red, massive at base, extensive fracturing at the top	0.75	7.25
8. Sandstone, yellow, massive, very fine sand	1.10	6.50
7. Siltstone and shale, dark-gray at basal contact, light-gray, very fine sand at top 5-cm of the bed	0.62	5.40
6. Limestone, bed #1, greenish-gray to medium-gray, some highly fossiliferous areas, mostly massive, some indistinct layering; gastropods are mm to cm in size, intact and partially fragmented, black in color, weathers pale yellow to pale olive	0.08	4.78
5. Shale, dark-gray grading to light-gray then dark-gray at the upper contact (10-cm) with limestone bed #1	1.48	4.70
4. Sandstone, red, massive, well-sorted, fine- to medium-grained	0.02	3.22
3. Shale, olive-gray, silty in places	0.80	3.20
2. Sandstone, yellowish-brown, fine to very fine sand, friable, with some 8- to 15-cm discontinuous coarser sandstone lenses that fine towards the top with 2-mm muscovite flakes, irregular upper contact	1.85	2.40
1. Sandstone, light-gray, interbedded with at least 3 layers of yellowish-brown to dark-grayish-brown silt and very fine sand, bed covered in places	0.55	0.55
Total thickness of section 3		18.25+

Base of section: terminated at covered interval in a portion of the main body of the Wasatch Formation, higher than base of section 2. Covered below.

Section 4

Stratigraphic section was measured from the NW 1/4, NW 1/4, SE 1/4 sec. 12, T. 17 N., R. 100 W., Sand Butte Rim NW 7-1/2 minute quadrangle, Sweetwater County, Wyoming to the top of section, located in the NW 1/4, SE 1/4, SE 1/4 sec. 12, T. 17 N., R. 100 W., Antelope Flats 7-1/2 minute quadrangle, Sweetwater County, Wyoming.

Top of section: Unit forms ridge top with overlying rocks separated by a large saddle area in a portion of the main body of the Wasatch Formation.

	Unit Thickness (Meters)	Cumulative Thickness (Meters)
29. Limestone, bed #3, very pale-grayish-orange, massive, recrystallized; rare fossils, weathers gray	0.10+	17.90+
28. Shale, poorly exposed	0.25	17.80
27. Sandstone, reddish-brown, fractured	0.15	17.55
26. Siltstone, yellowish-gray, loose, not well cemented	0.20	17.40
25. Shale, poorly exposed	0.70	17.20
24. Sandstone and siltstone, mottled light-brown and yellow, massive, very fine sand; weathers medium dark brown	0.76	16.50
23. Shale, poorly exposed	0.10	15.74
22. Sandstone and siltstone, mottled light-brown and very light-gray, massive, very fine sand; weathers dark brown	0.04	15.64
21. Shale, poorly exposed	2.10	15.60
20. Sandstone, yellow, red at upper surface	0.80	13.50
19. Shale, mostly covered, grading to very fine and fine sandstone, massive; irregular upper contact	0.80	12.70
18. Sandstone, gray, dark-red at the top	0.20	11.90
17. Siltstone and sandstone, very fine sand, noncalcareous	0.10	11.70
16. Shale, gray, mostly covered	1.10	11.60
15. Sandstone, light-gray to yellow, blocky	0.50	10.50
14. Sandstone, yellow, laminations and cross-beds, non-calcareous, fine to very fine sand	1.00	10.00
13. Covered	2.02	9.00
12. Limestone, bed #2, pale- to very pale-grayish-orange and very pale-yellowish-brown, massive; moderately abundant, small to large gastropods; fractured, weathers grayish brown to light brownish gray	0.18	6.98

	Unit Thickness (Meters)	Cumulative Thickness (Meters)
11. Shale, gray, dark-gray at the top	2.30	6.80
10. Sandstone, reddish-brown	0.10	4.50
9. Siltstone, pale-reddish-brown	0.20	4.40
8. Shale, alternating dark- and light-gray	0.88	4.20
7. Limestone, bed #1, very light- to light-gray, with areas of medium-dark-gray (corresponds with highly fossiliferous areas), mostly massive, some indistinct layering; gastropods are mm in size, intact, partially fragmented, black in color, bed grades to a very light gray towards top of bed, weathers pale yellow to light dusky yellow	0.02	3.32
6. Shale, dark-gray	0.10	3.30
5. Siltstone and sandstone, light-gray to olive-brown, which grades into a shale, upper contact grades back into siltstone and sandstone that is gray to olive-gray	2.25	3.20
4. Sandstone, reddish-brown, some cross-laminations, erosional lower contact	0.25	2.95
3. Siltstone, light-gray, grades into very fine and fine sand	0.70	2.70
2. Sandstone, gray to pale-yellow	0.10	2.00
1. Shale, gray, flaky, grading to siltstone at upper contact, slightly calcareous, highly fractured	1.90	1.90
 Total thickness of section 4		17.90+

Base of section: terminated at the top of a flaky, red-brown shale bed, probably higher than the base of section 3.

APPENDIX B. X-RAY DIFFRACTION DATA

HEIGHT of LARGEST PEAK for MINERALS

Limestone bed	Sample #	Calcite	Dolomite	Quartz	Feldspars		
					Albite	Microcline	Orthoclase
# 1	1	86	ND	1	<1	ND	ND
	2	84	ND	ND	ND	ND	ND
	3	84	ND	ND	ND	ND	ND
	4	87	<1	7	ND	ND	4
	5	92	ND	5	ND	ND	ND
	6	98	ND	2	ND	ND	ND
	7	102	ND	4	ND	ND	ND
	8	100	ND	5	ND	ND	ND
	9	57	2	27	3	ND	4
	10	92	3	44	8	ND	4
	11	105	ND	5	ND	ND	2
	12	68	3	81	5	ND	ND
	13	104	ND	5	1	ND	ND
# 2	14	82	1	20	4	ND	2
	15	75	ND	10	3	ND	2
	16	86	3	31	8	ND	4
	17	84	ND	21	5	ND	2
	18	93	5	14	1	ND	ND
	19	90	ND	20	4	ND	2
	20	80	ND	2	ND	ND	ND
	21	93	ND	2	1	ND	ND
	22	92	ND	3	ND	ND	5
	23	90	ND	4	ND	ND	ND
	24	94	ND	<1	ND	ND	ND
	25	74	3	36	7	ND	5
	26	79	ND	4	1	ND	ND
	27	102	ND	2	ND	ND	ND
	28	68	ND	4	2	ND	ND
	29	101	ND	1	ND	ND	ND

EXPLANATION

ND = not detected

APPENDIX B. X-RAY DIFFRACTION DATA (continued)

Limestone bed #	Sample #	HEIGHT of LARGEST PEAK for MINERALS					
		Calcite	Dolomite	Quartz	Feldspars		
					Albite	Microcline	Orthoclase
# 3	30	87	ND	7	2	ND	ND
	31	100	ND	2	2	ND	ND
	32	100	ND	1	ND	ND	ND
	33	105	ND	1	ND	ND	ND
	34	102	ND	8	ND	ND	ND
	35	102	ND	2	ND	ND	ND
	36	100	ND	<1	ND	ND	ND
	37	103	ND	2	ND	ND	ND
	38	102	ND	ND	ND	ND	2
	39	105	ND	<<1	ND	ND	ND
	40	102	ND	<1	ND	ND	ND
	41	99	ND	1	ND	ND	ND
	42	103	ND	2	ND	ND	ND
	43	61	43	<1	ND	ND	ND
	44	71	26	1	ND	ND	ND
	45	93	4	<1	ND	ND	ND

EXPLANATION

ND = not detected

APPENDIX C. INSOLUBLE RESIDUE DATA

BED #	Sample Number	RESIDUE %			Average	Standard Deviation	Standard Deviation as % of Average
		Run 1	Run 2	Run 3			
1	1	5.170	5.407	0.850	3.809	2.565	67.3
	2	1.348	0.757	0.566	0.890	0.408	45.8
	3	1.611	1.820	2.468	1.966	0.447	22.7
	4	6.883	5.173	4.953	5.670	1.057	18.6
	5	5.522	5.045	5.346	5.304	0.241	4.5
	6	4.966	5.358	4.366	4.897	0.500	10.2
	7	2.939	2.808	3.164	2.970	0.180	6.1
	8	9.711	10.649	9.637	9.999	0.564	5.6
	9	30.622	31.893	30.976	31.164	0.656	2.1
	10	29.858	28.568	31.096	29.841	1.264	4.2
	11	4.170	5.323	5.399	4.964	0.689	13.9
	12	39.095	41.666	43.642	41.468	2.280	5.5
	2	13	5.432	5.084	5.122	5.213	0.191
14		21.654	19.526	20.806	20.662	1.071	5.2
15		10.195	9.602	18.040	12.612	4.710	37.3
16		32.763	34.335	31.338	32.812	1.499	4.6
17		24.125	21.518	23.387	23.010	1.344	5.8
18		6.999	12.412	11.338	10.250	2.866	28.0
19		18.115	21.923	22.370	20.803	2.338	11.2
20		6.398	6.797	5.044	6.080	0.919	15.1
21		5.356	6.604	5.032	5.664	0.830	14.7
22		2.888	3.531	2.473	2.964	0.533	18.0
23		4.533	5.213	2.136	3.961	1.616	40.8
24		3.736	4.668	3.773	4.059	0.528	13.0
25		32.398	31.425	30.437	31.420	0.981	3.1
26		6.996	6.848	5.698	6.514	0.711	10.9
27	24.657	24.879	25.198	24.911	0.272	1.1	
3	28	7.546	5.832	6.513	6.630	0.863	13.0
	29	5.232	6.983	7.149	6.455	1.062	16.5
	30	4.797	5.637	5.338	5.257	0.426	8.1
	31	3.356	5.253	2.894	3.834	1.250	32.6
	32	1.519	2.268	0.638	1.475	0.816	55.3
	33	2.591	1.706	1.057	1.785	0.770	43.1
	34	5.472	4.962	7.832	6.089	1.531	25.1
	35	0.982	1.215	0.949	1.049	0.145	13.8
	36	0.693	0.382	0.824	0.633	0.227	35.9
	37	1.671	1.798	1.538	1.669	0.130	7.8
	38	1.913	1.438	0.517	1.289	0.710	55.0
	39	0.303	0.831	0.634	0.589	0.267	45.3
	40	3.281	2.196	2.057	2.511	0.670	26.7
	41	1.238	1.143	2.280	1.554	0.631	40.6
	42	2.887	3.427	2.737	3.017	0.363	12.0
	43	5.453	4.930	1.832	4.072	1.957	48.1
	44	2.361	2.341	1.317	2.006	0.597	29.8
	45	2.334	2.418	1.323	2.025	0.609	30.1

APPENDIX D. PETROGRAPHIC DATA (continued 2)

SAMPLE #	Limestone bed #3																				
	FOSSIL: Ostracods	FOSSIL: Gastropods	FOSSIL: Pelecypods	TOTAL FOSSILS (F)	PELLETS (P)	TOTAL ((F) + (P))	INTRACLASTS (I)	COATED GRAINS (C)	TOTAL ((I) + (C))	MATRIX (M)	CEMENT (cmt)	TOTAL ((M) + (cmt))	TOTAL CARBONATE (F + P + I + C + M + cmt)	QUARTZ	FELDSPARS	APATITE (bone)	ROCK FRAGMENTS	OTHER	TOTAL NON-CARBONATE GRAINS	PORE SPACE	GRAND TOTAL
30	0	2	84	86	0	86	0	0	0	203	6	209	295	0	0	4	0	0	4	1	300
31	0	77	0	77	1	78	0	0	216	0	216	294	0	0	0	0	0	0	3	3	300
32	0	77	2	79	0	79	1	1	218	2	220	300	0	0	0	0	0	0	0	0	300
33	0	101	0	101	0	101	0	0	190	1	191	292	0	0	0	7	0	0	7	1	300
34	0	70	13	83	0	83	1	1	199	3	202	286	5	3	0	1	0	1	9	5	300
35	0	52	12	64	0	64	1	1	221	3	224	289	0	2	1	0	0	0	3	8	300
36	0	53	4	57	1	58	0	0	238	3	241	299	1	0	0	0	0	0	1	0	300
37	0	22	7	29	0	29	1	1	218	6	224	254	21	14	0	0	0	1	36	10	300
38	1	104	1	106	0	106	0	0	184	3	187	293	1	1	0	0	0	0	2	5	300
39	0	74	12	86	0	86	1	2	204	0	204	292	0	0	1	0	0	1	2	6	300
40	0	98	6	104	0	104	1	1	194	0	194	299	0	0	0	0	0	0	0	1	300
41	0	45	0	45	0	45	1	2	253	0	253	300	0	0	0	0	0	0	0	0	300
42	0	107	0	107	0	107	1	1	184	6	190	298	2	0	0	0	0	0	2	0	300
43	0	37	0	37	0	37	0	0	262	0	262	299	0	0	0	0	0	1	1	0	300
44	0	29	0	29	0	29	1	1	258	7	265	295	2	1	1	0	0	1	5	0	300
45	0	59	0	59	0	59	2	2	237	0	237	298	1	0	0	0	0	0	1	1	300